UNSW THE UNIVERSITY OF NEW SOUTH WALES

AI in Medicine: Making impact in Clinical Practice

Never Stand Still | Faculty of Engineering | School of Computer Science and Engineering

Dr Sonit Singh

Computer Vision Group, Artificial Intelligence Theme
School of Computer Science and Engineering
Faculty of Engineering
The University of New South Wales, Sydney, Australia
sonit.singh@unsw.edu.au

Recent breakthroughs: AI, ML, DL

- **Artificial Intelligence (AI)**: development of smart systems and machines that can carry out tasks that typically require human intelligence
- **Machine Learning**: creates algorithms that can learn from data and make decisions based on patterns observed. Requires human intervention when decision is incorrect
- **Deep Learning**: uses complex and deep artificial neural networks to reach accurate conclusions without human intervention. Requires large-scale annotated data to train.

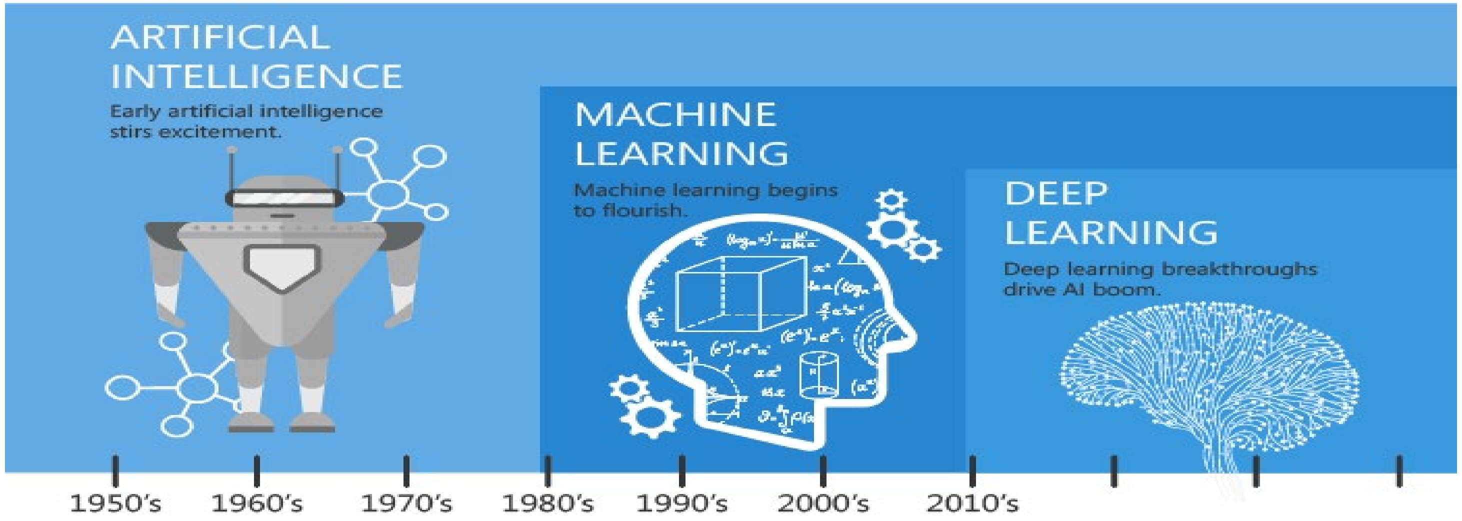

The Need: Augmented Intelligence

➢ Humans + Computers can achieve better performance than either alone

Harvard Business Review

Innovation | AI Will Change Radiology, but It Won't Replace Radiologists

AI Will Change Radiology, but It Won't Replace Radiologists

by Thomas H. Davenport and Keith J. Dreyer, DO

March 27, 2018

Augmentation or Companionship

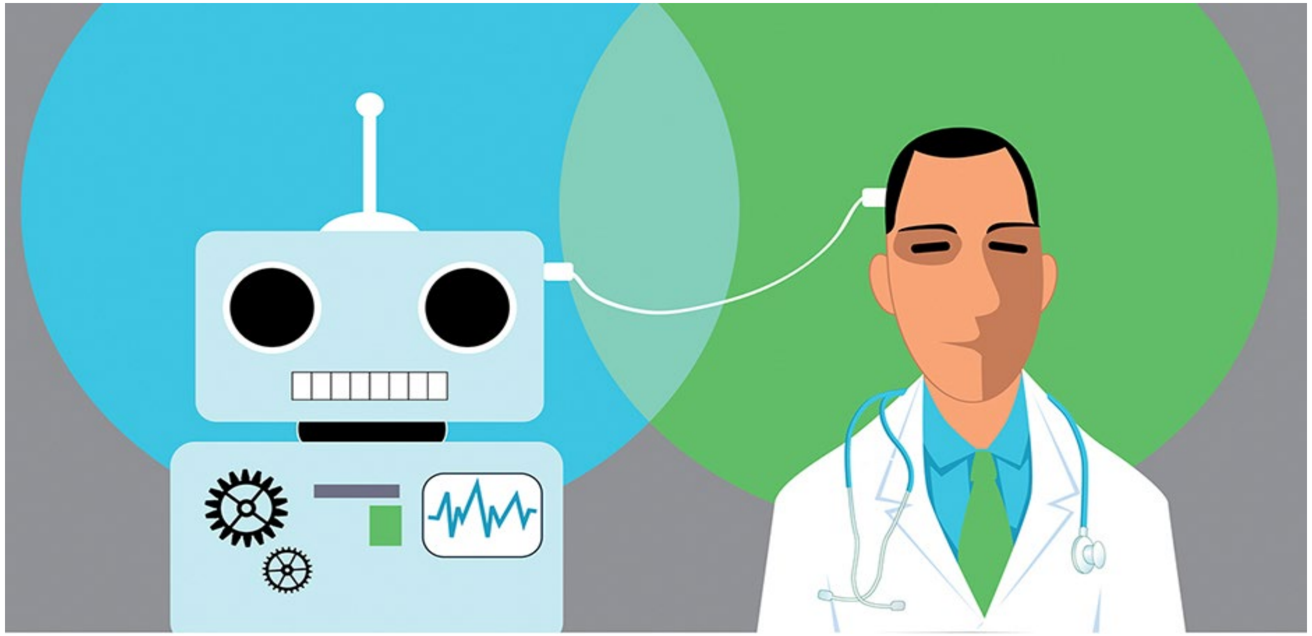

In contrast to automation, augmentation presumes that smart humans and smart machines can coexist and create better outcomes than either could alone. AI systems may perform some health care tasks with limited human intervention, thereby freeing clinicians to perform higher-level tasks."

Image Credit: https://www.ups.com/us/en/services/knowledge-center/article.page?name=3-principles-for-bringing-augmented-intelligence-to-life-sciences&kid=cd1a6e81

Convolutional Neural Networks (CNNs)

- A class of deep neural networks suitable for processing 2D/3D data. For e.g., Images and Videos
- CNNs can capture high-level representation of images/videos which can be used for end-tasks such as classification, object detection, segmentation, etc.
- A range of CNNs improving over the years

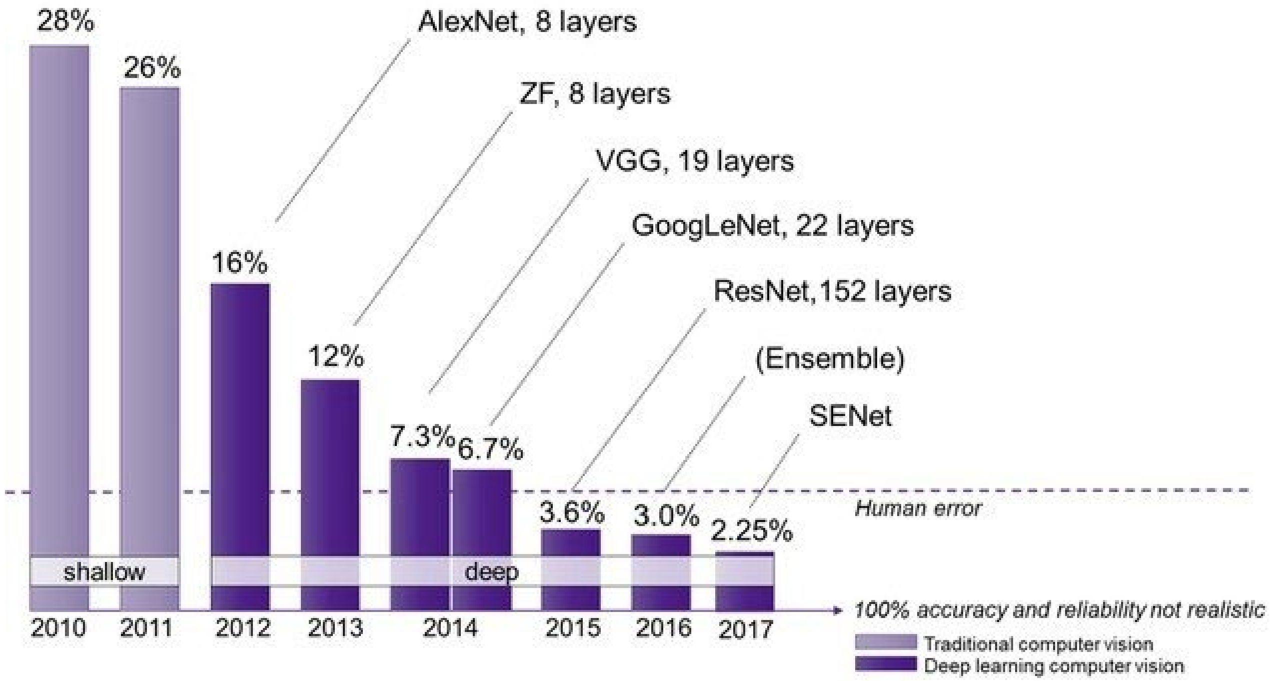

Source: Convolutional Neural Networks. https://medium.com/@rajat.k.91/convolutional-neural-networks-why-what-and-how-f8f6dbebb2f9

CNN Architecture

- A typical CNN architecture consists of the following layers:
  - Convolution layer
  - ReLU layer (non-linearity)
  - Pooling layer
  - Flattening
  - Fully-connected layer
  - Output layer

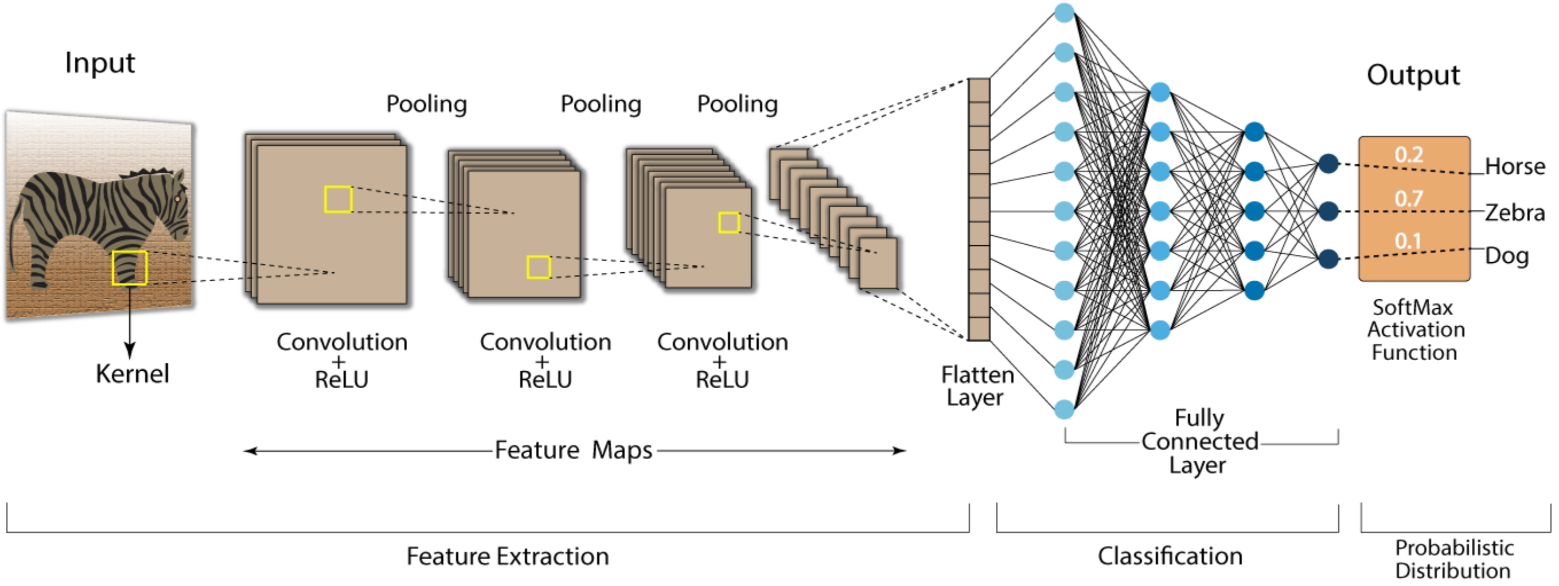

- There can be multiple steps of convolution followed by pooling, before reaching the fully connected layers.

Vision tasks

- Image classification: Assigning a label or class to an image
- Object detection: Locate the presence of objects with a bounding box and class of the located objects in an image
- Semantic segmentation: Label every pixel (pixel-wise classification)
- Instance segmentation: Differentiate instances

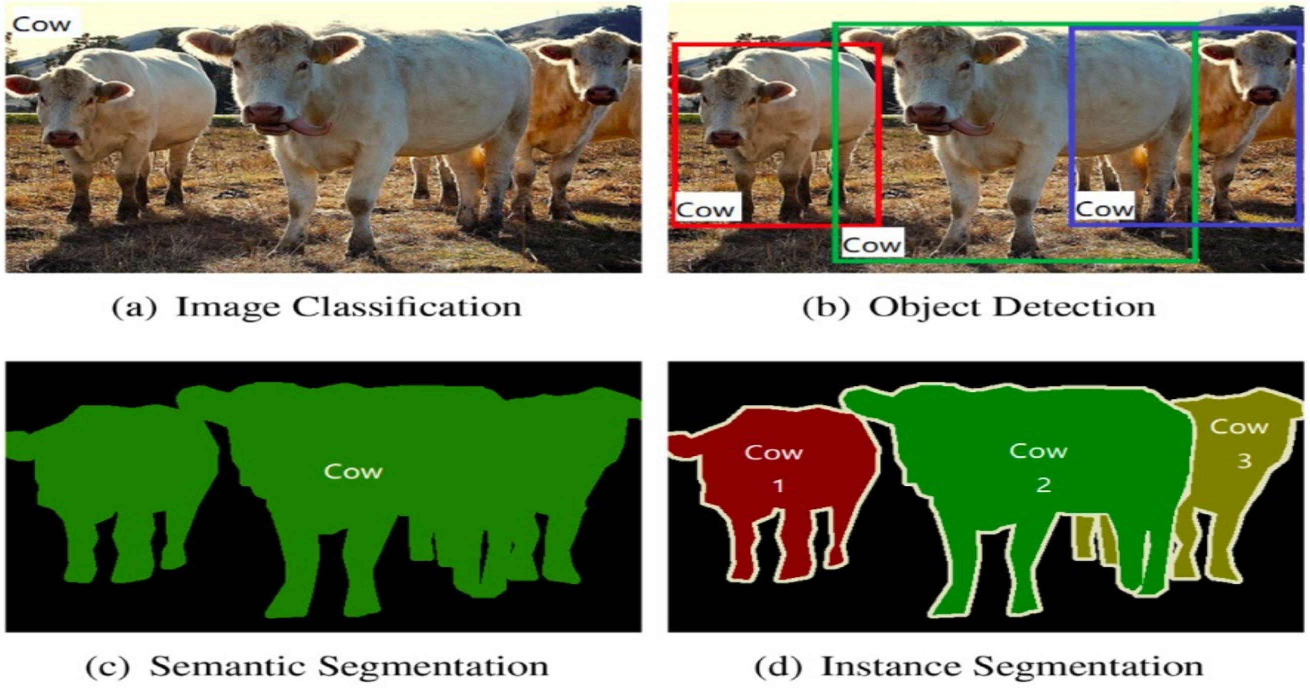

Image Credit: https://medium.com/@deepeshandphone/history-of-deep-learning-on-object-detection-5c94f63ec475

Object detection with Faster R-CNN

- Determine "what" and "where"
  - regress the coordinates of object and classify it
- Region Proposal: R-CNN, Fast R-CNN, Faster R-CNN, Mask R-CNN
  - First propose the regions likely to include objects and second classify the regions and regress the BBOX
- R-CNN: Detect RoI by Selective Search (SS) on images, resize the regions to fixed size and let them flow into CNN respectively, and classify them into the classes by SVM

R-CNN: ***Regions with CNN features***

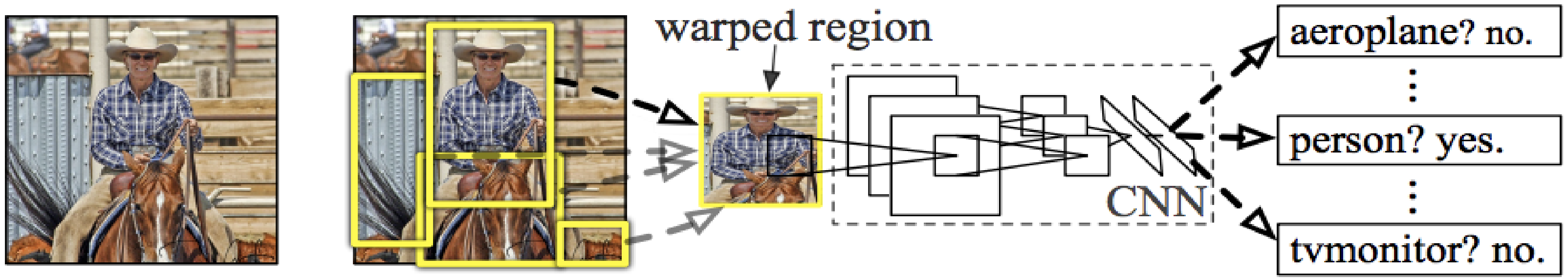

1. Input image
2. Extract region proposals (~2k)
3. Compute CNN features
4. Classify regions

Object detection with Faster R-CNN

- R-CNN Issues
  - A split between region proposal and classification
  - Too slow selective search (can't be used in real-time)
- Fast R-CNN: Do convolution first and then selective search. Adopted RoI pooling to crop fixed vector from the feature map.
- Fast R-CNN:
  - RoI Pooling
  - Speeded up the forward propagation by sharing convolution

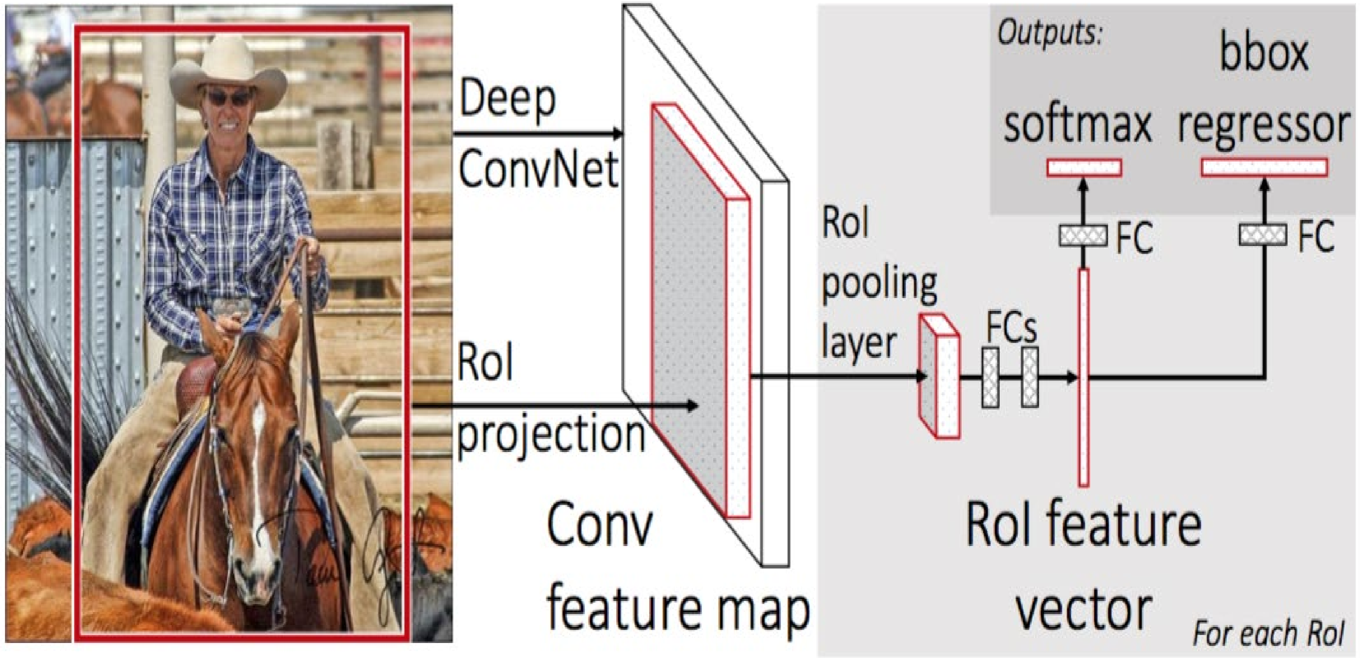

Image Credit: Grishick (2015). Fast R-CNN. ICCV 2015.

Object detection with Faster R-CNN

- Fast R-CNN Issues
  - A split between region proposal and classification was not improved
  - Selective Search still too slow
- Faster R-CNN
  - Adopted Region Proposal Network (RPN) and abolish Selective Search
  - Achieved high performance and high speed

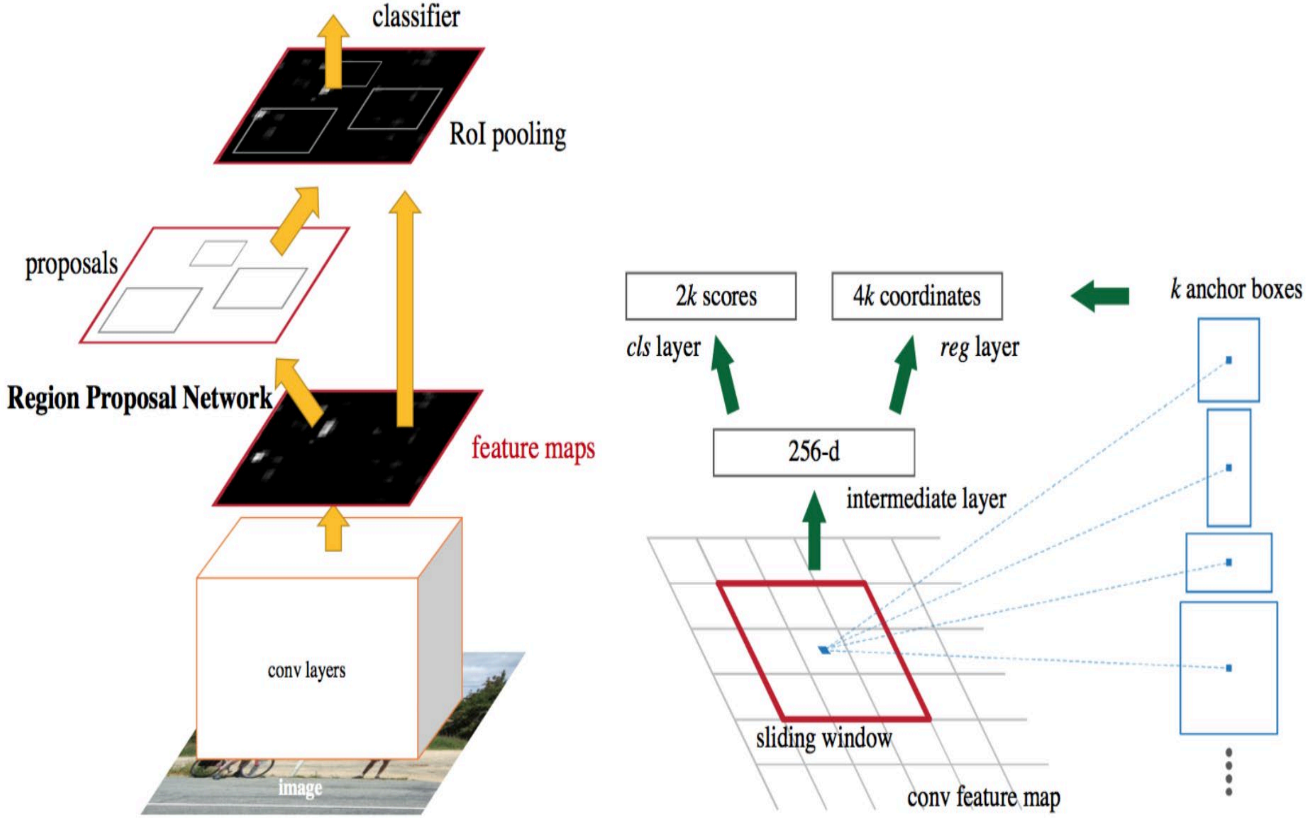

Biomedical Image Segmentation with U-net

- U-net learns segmentation in an end-to-end setting
- Proven to be very powerful segmentation tool in scenarios with limited annotated data
- Doesn’t contain any fully connected layers

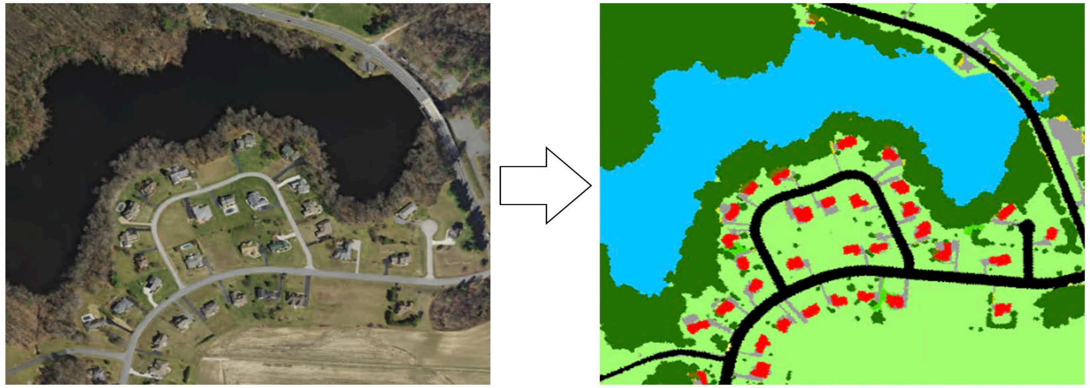

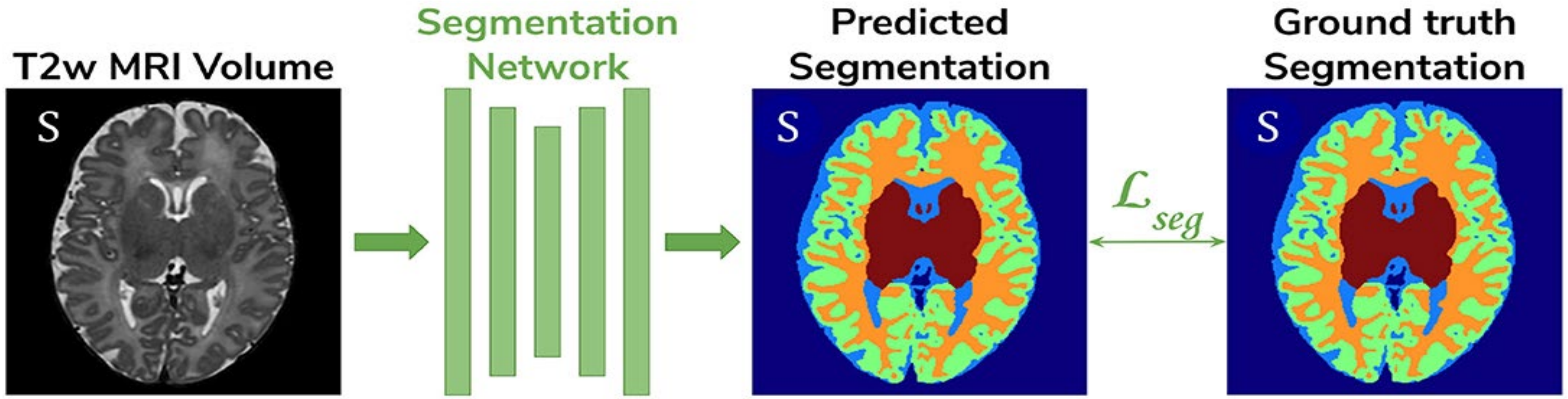

U-net Architecture

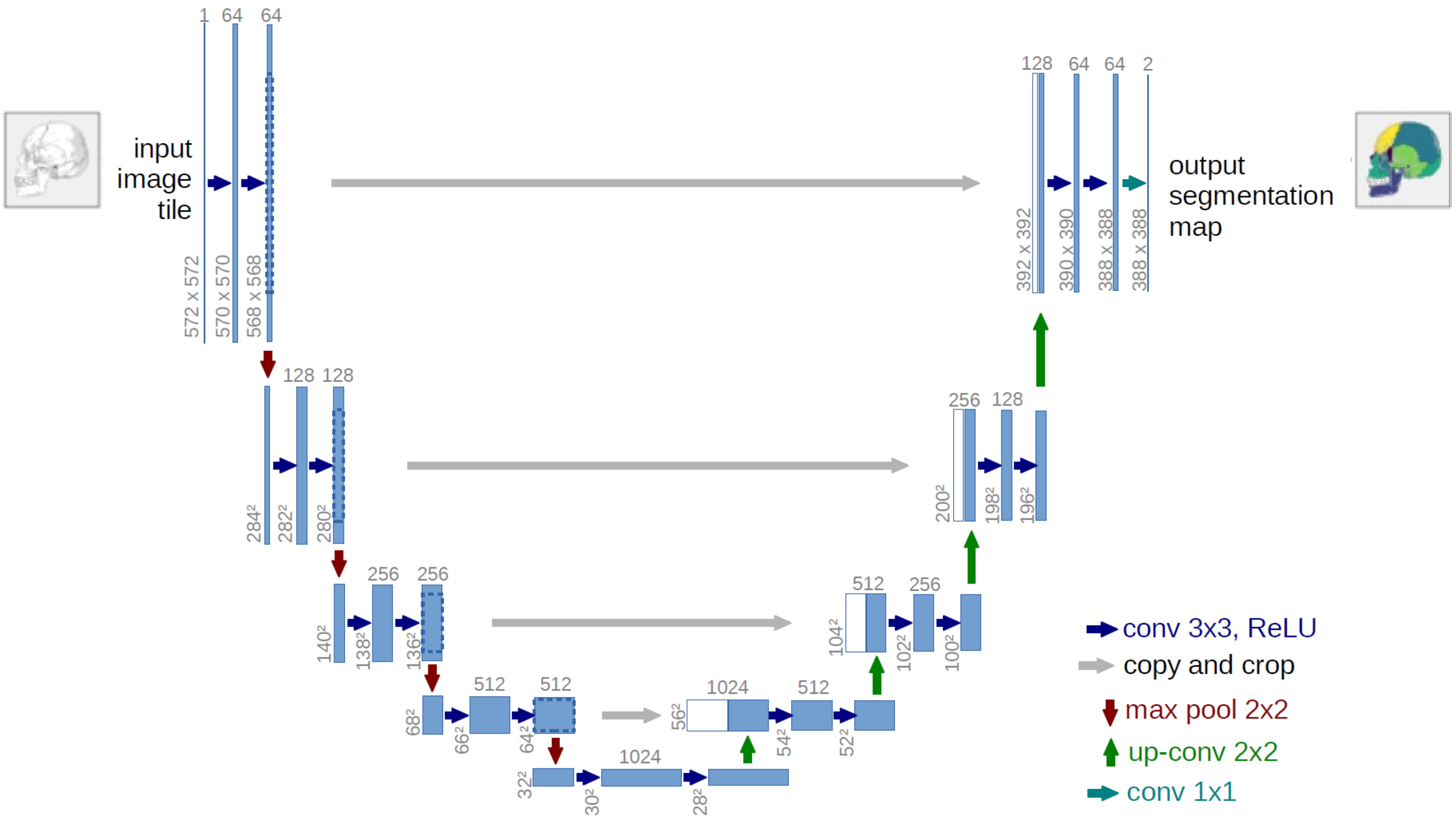

Source: Ronneberger et al. (2015). U-net: Convolutional Networks for Biomedical Image Segmentation. MICCAI 2015.

Case Study: Automated Analysis of 4D Fetal Echocardiogram*

- Problem Statement

Given a 4D Fetal echocardiogram, segment the four cardiac chambers and the mitral and tricuspid annulus, creating a 3D model of the fetal heart at End-Diastole. Compute essential biometrics to assess the well-being of the fetus from this model by tracking it over the entire cardiac cycle.

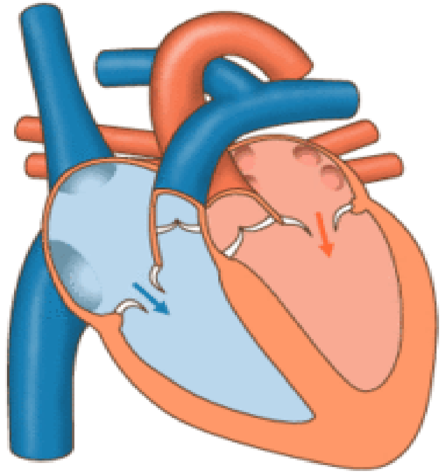

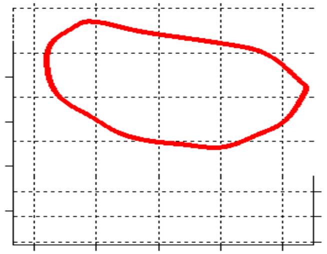

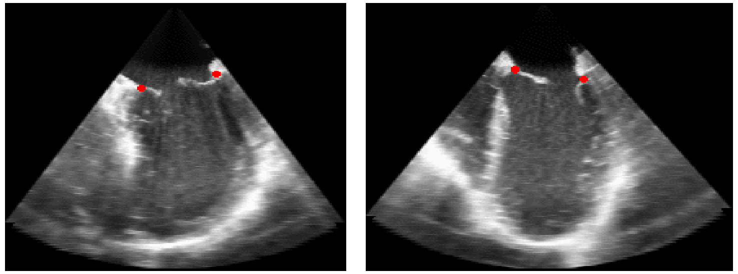

Adult Annulus Segmentation [1].

*Joint work with Philip, Ferrieira, Tomar, Chawla, Welsh, Stevenson

Background

- Heart is the **first functional organ** that develops in a fetus.
- Starts beating by **Week 4**
- The heart has four chambers, two atria (left and right atrium) and two ventricles (left and right ventricle)
- The fetus has a **parallel circulation** compared to the serial system in adults – because lungs are not functional
- **Mitral (Bicuspid) Valve** (MV): opens during diastole, allows blood to flow down from the LA to the LV and closes during systole to prevent the blood from flowing back to the LA
- **Tricuspid Valve** (TV): opens during diastole, allows blood to flow down from the RA to the RV and closes during systole to prevent the blood from flowing back to the RA

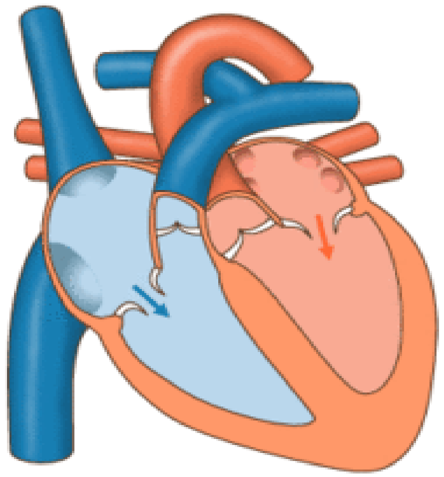

Background

- We are interested in the **Annulus region**, a saddle shaped fibrous ring, which moves up and down during a cardiac cycle.
- The annulus controls the opening and closing of the valves.
- The vertical displacement of the **mitral annulus** is termed **MAPSE**
- The same of the **tricuspid annulus** is termed **TAPSE**

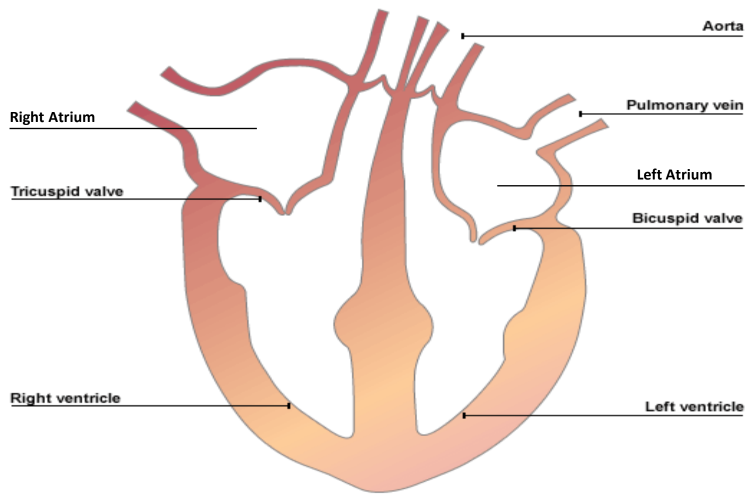

Four chambers of the heart.

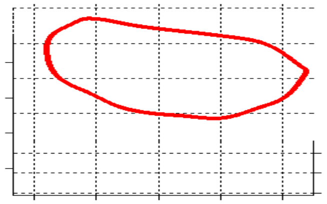

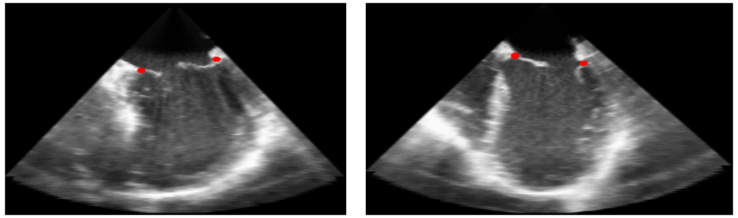

Adult Annulus Segmentation [1].

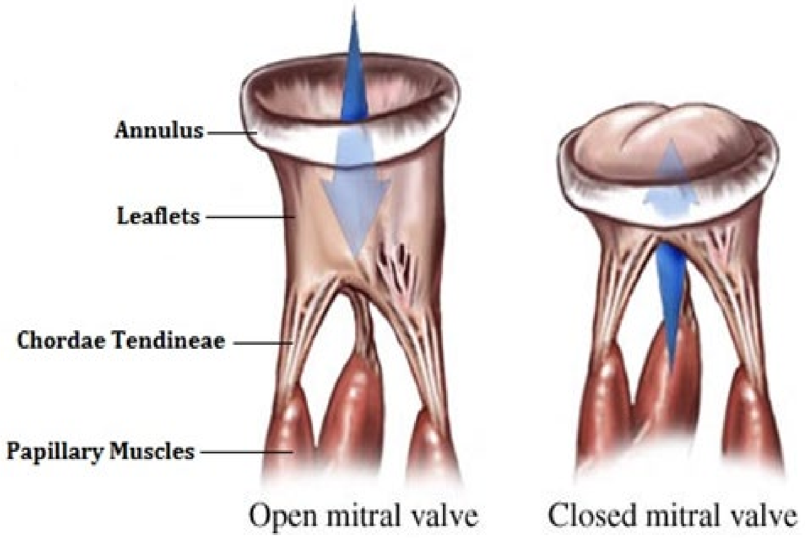

Mitral Valve showing the fibrous annulus ring surrounding the leaflet.

*Joint work with Philip, Ferrieira, Tomar, Chawla, Welsh, Stevenson

Datasets

Dataset-1

- 295 Ultrasound Volumes (Acquired by 3 operators)
  - 95 foetuses (Gestational Age: 20-37 weeks)
  - **4D** data (3D + time)
  - Annotations available:
    - TAPSE/MAPSE measurements by 3 operators (3 measurements each)
    - Tricuspid/Mitral annuli annotated on 169 * 3D volumes

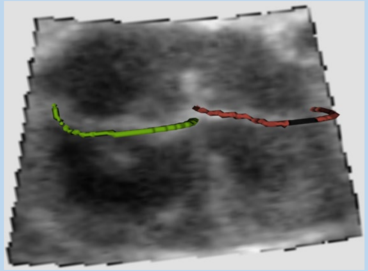

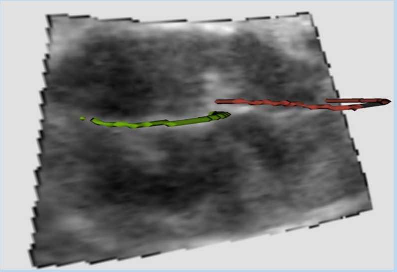

Dataset-2

- 385 Ultrasound Volumes (Acquired by 1 operator)
  - 32 foetuses
  - **4D** data (3D + time)
  - Probe used for data acquisition: E8-STIC, E10-STIC, E10-eSTIC
  - Annotations available:
    - 6 classes: Left Atrium (LA), Left Ventricle (LV), Mitral Annulus (MA), Right Atrium, Right Ventricle, Tricuspid Annulus (TA)
    - 2 Annotators
    - 30 Volumes (each annotated in triplicates by each annotator)

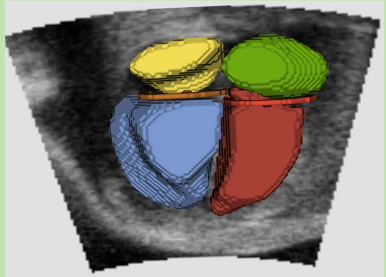

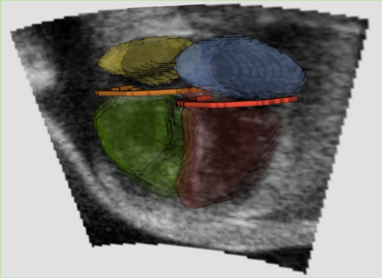

Data Preparation

- **Quality Scoring System –** manually evaluated (out of 8)
- Volumes with a score >= 4, selected

Scoring Parameter		Score
Visibility of	4 Chamber View	1
	Aorta	1
	Moderator band	1
	Whole heart	1
Noise level	High/Moderate/Low	1/2/3
Re-orientation required		1
TOTAL		**8**

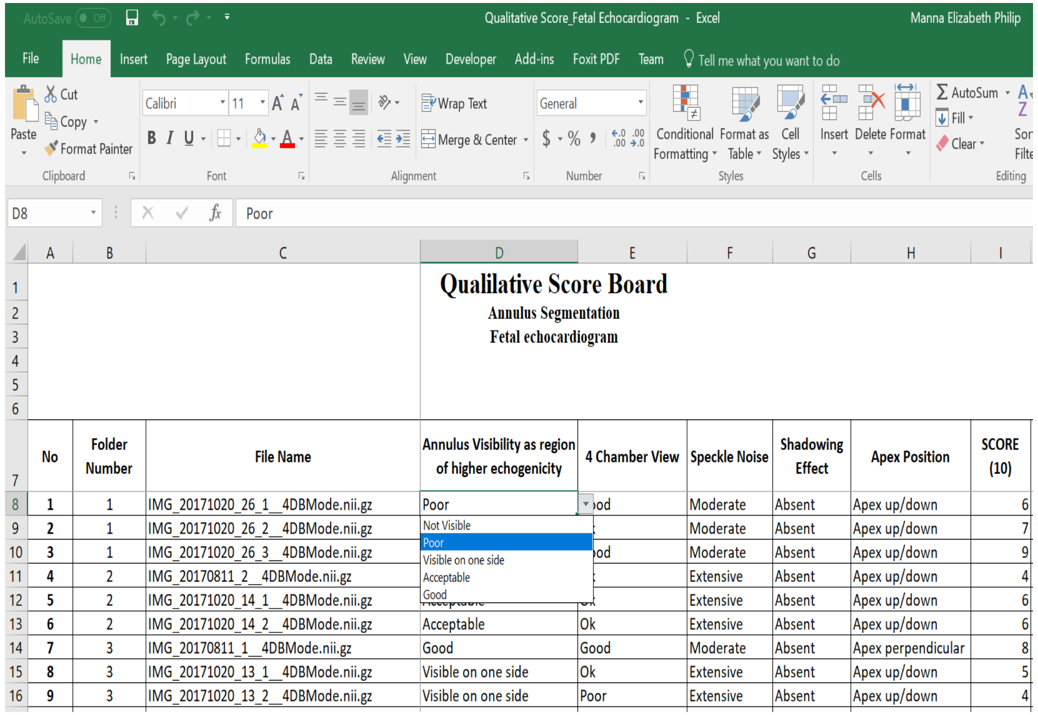

No	Folder Number	File Name	Annulus Visibility as region of higher echogenicity	4 Chamber View	Speckle Noise	Shadowing Effect	Apex Position	SCORE (10)
1	1	IMG_20171020_26_1__4DBMode.nii.gz	Poor	[illegible]	Moderate	Absent	Apex up/down	6
2	1	IMG_20171020_26_2__4DBMode.nii.gz	Not Visible	[illegible]	Moderate	Absent	Apex up/down	7
3	1	IMG_20171020_26_3__4DBMode.nii.gz	Poor	[illegible]	Moderate	Absent	Apex up/down	9
4	2	IMG_20170811_2__4DBMode.nii.gz	Visible on one side	[illegible]	Extensive	Absent	Apex up/down	4
5	2	IMG_20171020_14_1__4DBMode.nii.gz	Acceptable	[illegible]	Extensive	Absent	Apex up/down	6
6	2	IMG_20171020_14_2__4DBMode.nii.gz	Acceptable	Ok	Extensive	Absent	Apex up/down	6
7	3	IMG_20170811_1__4DBMode.nii.gz	Good	Good	Moderate	Absent	Apex perpendicular	8
8	3	IMG_20171020_13_1__4DBMode.nii.gz	Visible on one side	Ok	Extensive	Absent	Apex up/down	5
9	3	IMG_20171020_13_2__4DBMode.nii.gz	Visible on one side	Poor	Extensive	Absent	Apex up/down	4

1. Annulus Segmentation

- U-Net architecture used to segment the tricuspid and mitral annulus
- **Dice Similarity Coefficient** (DSC) values of **0.78** for **Tricuspid Annulus** (TA) segmentation and **0.77** for **Mitral Annulus** (MA) segmentation were achieved.
- TAPSE/MAPSE Measurement
  - For TAPSE measurements, r=0.61 and RMSE=0.14 cm
  - For MAPSE measurements, r=0.30 and RMSE=0.18 cm
- This automated method can provide function cardiac assessment where training is limited and skills lacking
- **Presented @ IEEE ISBI 2019**

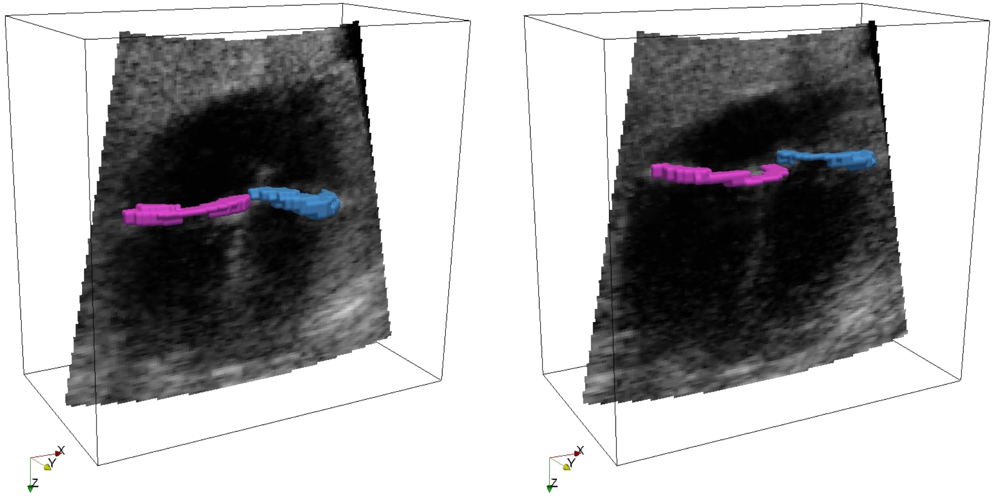

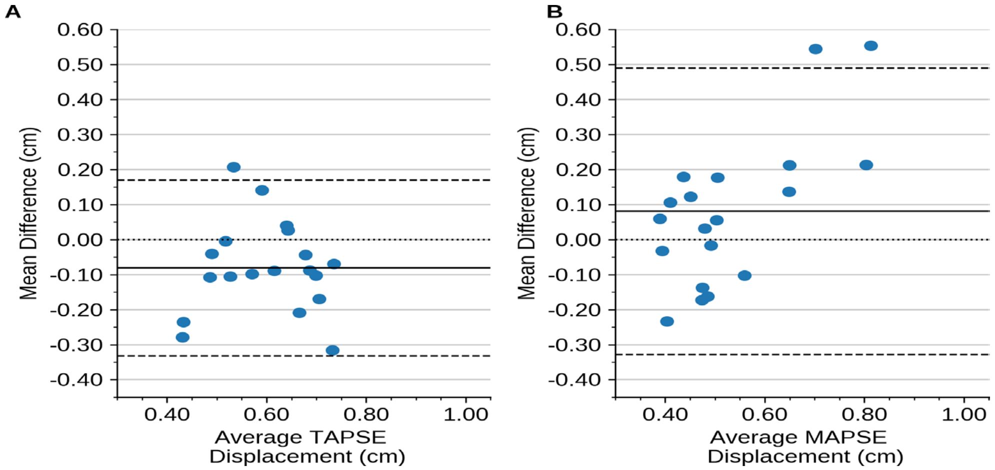

Bland-Altman plots comparing automated TAPSE (A) and MAPSE (B) measurements to average expert measurement.

M. E. Philip, A. Sowmya, H. Avnet, A. Ferreira, G. Stevenson and A. Welsh, "Convolutional Neural Networks for Automated Fetal Cardiac Assessment using 4D B-Mode Ultrasound," *2019 IEEE 16th International Symposium on Biomedical Imaging (ISBI 2019)*, 2019, pp. 824-828, doi: 10.1109/ISBI.2019.8759377.

Annulus Segmentation - Issues

- Change in orientation of the heart due to fetal or probe movement
- Position of the SEPTUM
- Tracking not performed to confirm End-systole and End-diastole

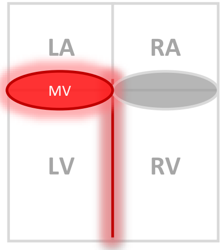

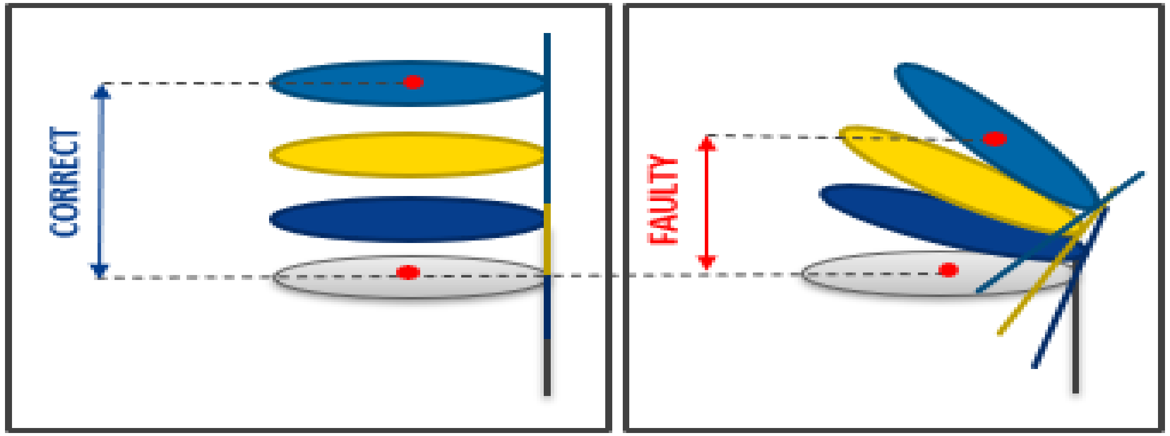

Figure : Schematic depicting need for Registration.

2. Whole Heart Segmentation

- Instead of identifying just the SEPTUM for orientation-problem redefined to obtain it as a by-product
- The heart is modelled consisting of:
  - Left and Right Atrium (LA, RA)
  - Left and Right Ventricles (LV, RV), and
  - Tricuspid and Mitral Annulus (TA, MA)
- Dataset-1 could not be used
  - Whole heart was not in view
  - Zoomed in version of the thorax

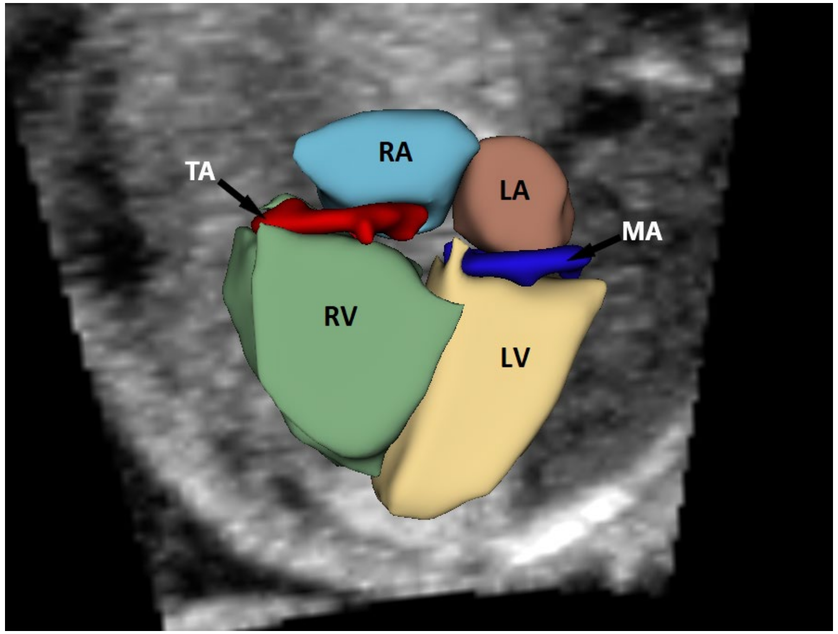

3D render of heart model, showing cardiac chambers and anuuli.

Datasets

- **Dataset-2**
- 385 Ultrasound Volumes (Acquired by 1 operator)
  - 32 foetuses
  - **4D** data (3D + time)
  - Probe used for data acquisition: E8-STIC, E10-STIC, E10-eSTIC
  - Annotations available:
    - 6 classes: Left Atrium (LA), Left Ventricle (LV), Mitral Annulus (MA), Right Atrium, Right Ventricle, Tricuspid Annulus (TA)
    - 2 Annotators
    - 30 Volumes (each annotated in triplicates by each annotator)

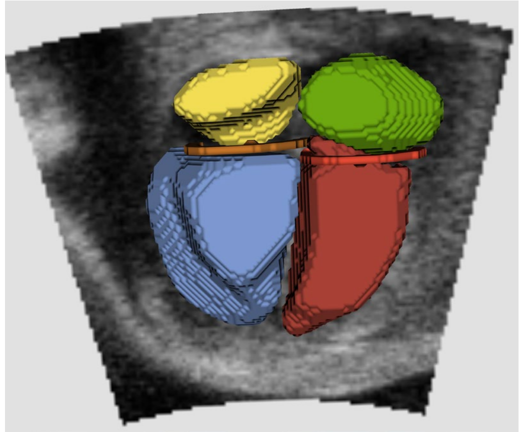

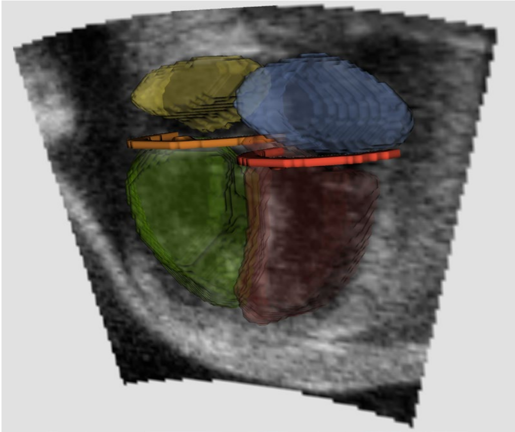

Issues

➢ Inter and Intra observer Variability

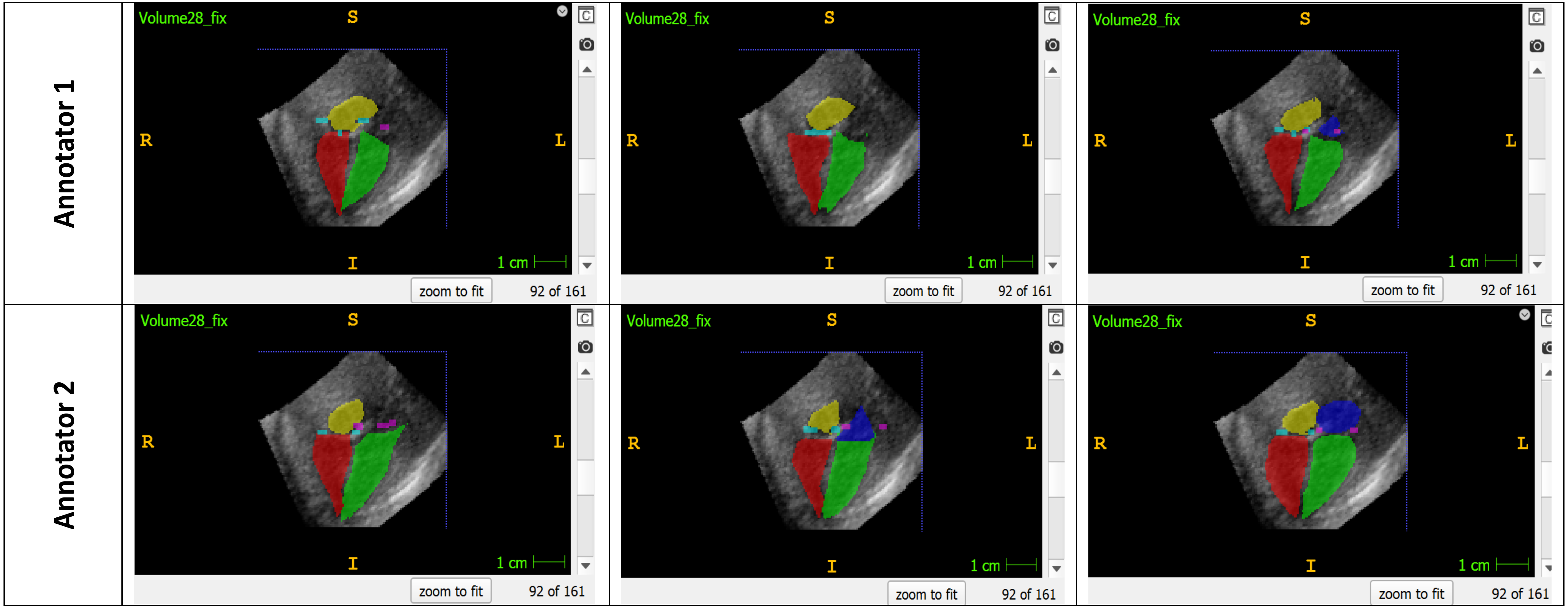

Architectures

- CNN based models:
  - U-Net
  - V-Net
  - Res-UNet

- Transformer-based models:
  - TransBTS
  - Unet-R

Training details

- Training data:

Number of patients	20
Total annotated ED volumes	30
Train volumes	25 (15 patients)
Training Patient IDs	0,2,3,4,5,6,8,9,13,14,24,26,27,28,30,31,35 (Fold 1)
Test volumes	5 (5 patients)
Test Patient IDs	1,7,10,25,32 (Fold 1)

- Training Parameters

Augmentation	Rotation at ±(3,6,9)°, Gaussian noise, Salt and Pepper noise
Training samples after augmentation	2100
Train/ Validation split	90/10
Epochs trained for	100
Optimizer	Adam
Learning rate	1e-4
Batch size	2
Data Size	64 *64 *64

Whole Heart Segmentation

1. Position Fixing

- Manually repositioned to
  - Apex down – flipping data up/down
  - Mitral Annulus visible on the right side – flipping data left/right

2. Localisation (along coronal axis)

- SVM classifier trained to classify coronal slices to foreground / background

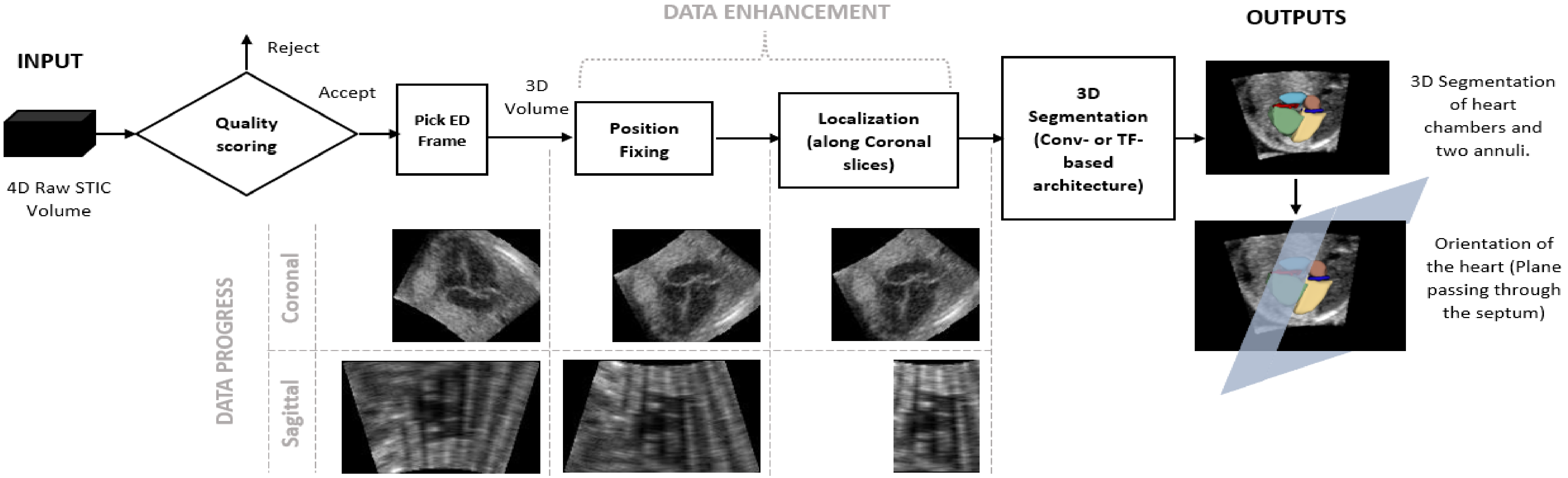

Flowchart outlining the proposed pipeline.

M. E. Philip *et al.*, "A Machine Learning Framework for Fully Automatic 3D Fetal Cardiac Ultrasound Evaluation," *2022 IEEE 19th International Symposium on Biomedical Imaging (ISBI)*, 2022, pp. 1-5, doi: 10.1109/ISBI52829.2022.9761613.

Segmentation results

- No matter the architecture used, clear **performance improvement with data enhancement**
- Performance improvement with data enhancement
  - **19%** ↑ in DSC for CNNs and a **16%** ↑ for transformer-based networks

Type	Architecture	Enh.	LV	RV	LA	RA	TA	MA
CNN-Based	U-Net [7]	A	0.60	0.67	0.40	0.69	0.48	0.37
		P	0.76	0.70	0.55	0.74	0.49	0.42
		L	**0.82**	**0.77**	**0.62**	**0.72**	**0.50**	**0.47**
	V-Net [13]	A	0.54	0.52	0.16	0.46	0.32	0.22
		P	0.64	0.65	0.38	**0.66**	**0.42**	**0.39**
		L	**0.74**	**0.73**	**0.44**	0.65	0.39	0.37
	Res U-Net [14]	A	0.36	0.32	0.26	0.48	0.24	0.16
		P	0.63	0.63	0.40	0.71	**0.42**	**0.37**
		L	**0.74**	**0.76**	**0.53**	**0.68**	**0.42**	0.36
TF-Based	TransBTS [15]	A	0.59	0.55	0.26	0.60	0.35	0.21
		P	0.74	0.69	0.59	**0.75**	**0.49**	**0.47**
		L	**0.80**	**0.78**	**0.65**	0.72	0.45	0.46
	U-NetR [16]	A	0.53	0.49	0.26	0.54	0.22	0.16
		P	0.66	0.62	**0.37**	**0.67**	**0.31**	**0.31**
		L	**0.70**	**0.67**	0.35	0.57	0.28	0.26

*Comparison of segmentation performance measured by DSC for multiple deep learning methods. Segmentation was performed using models trained on data using three different enhancements (**A** = Augmentation only; **P** = Augmentation + Position Fixing; **L** = Augmentation + Position Fixing + Localization). Best accuracy for each class is shown in bold*

M. E. Philip *et al.*, "A Machine Learning Framework for Fully Automatic 3D Fetal Cardiac Ultrasound Evaluation," *2022 IEEE 19th International Symposium on Biomedical Imaging (ISBI)*, 2022, pp. 1-5, doi: 10.1109/ISBI52829.2022.9761613.

Results analysis

- Physical size constraints reflected in segmentation results
  - Segmentation performance of ventricles > atria > annuli

- U-Net gave the best results
  - V-Net, UNet-R and Res-UNet highly sensitive to noise and fails to learn the general shape of the region
  - TransBTS very similar architecture to U-Net except for the transformer block – results very close to U-Net

- Mean DSC improvement after data enhancement:
  - U-Net: 0.12
  - V-Net: 0.18
  - Res-UNet: 0.28
  - TransBTS: 0.22
  - UNETR: 0.11

M. E. Philip *et al.*, "A Machine Learning Framework for Fully Automatic 3D Fetal Cardiac Ultrasound Evaluation," *2022 IEEE 19th International Symposium on Biomedical Imaging (ISBI)*, 2022, pp. 1-5, doi: 10.1109/ISBI52829.2022.9761613.

3. Automatic segmentation of human placenta in 3D Ultrasound

- The placenta is a critical and complex organ that provides oxygen and nutrition to the growing fetus and removes waste from its blood
- Fetal health strongly depends on the functionality of the placenta
- Any abnormality of the placenta could be harmful to the fetus and the mother
- Assessment of placenta in vivo across gestation is critical to understand placental structure, function, and development

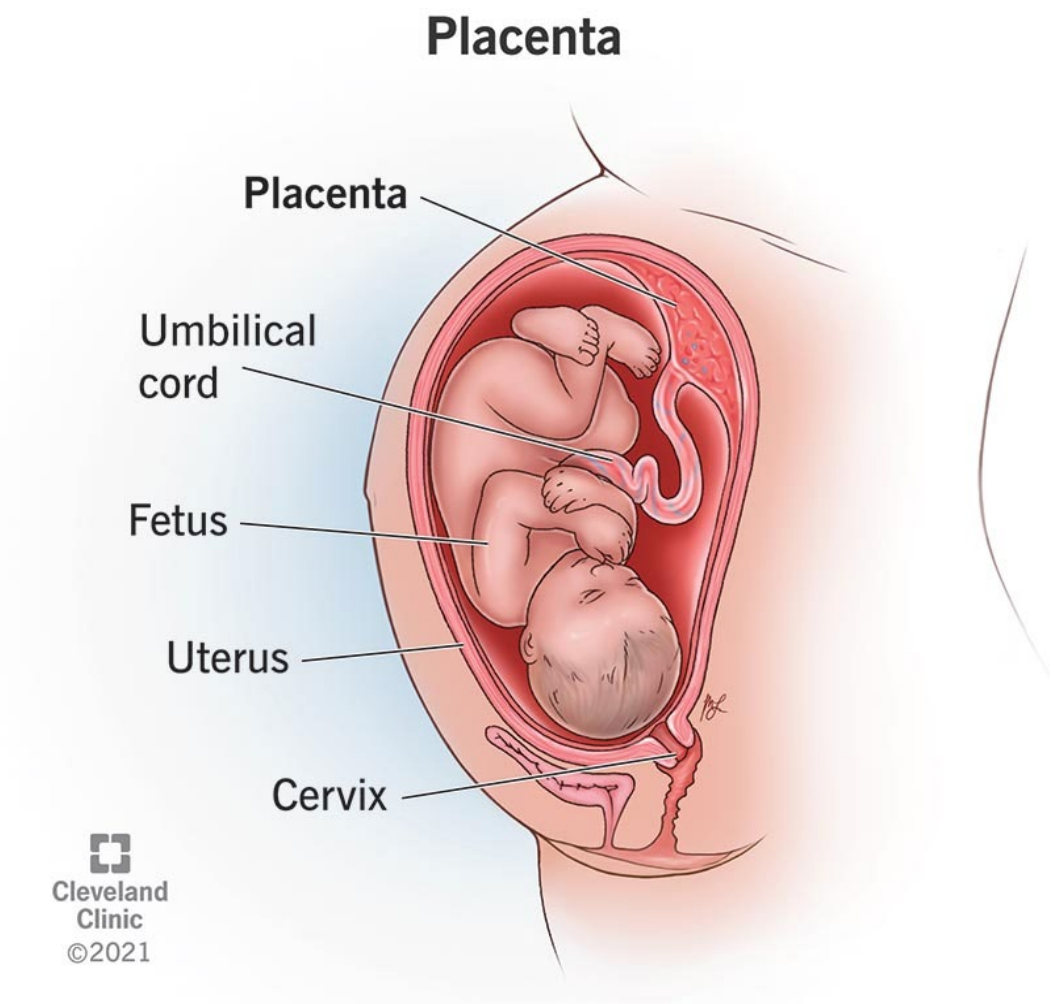

Need for 3D placenta volume segmentation

- 2D US is the standard clinical imaging modality used for accessing placental health and diagnosis of its abnormalities
- In 2D US imaging, physician create 3D model in their mind and subjectively determine volume, location, and features of the placenta – challenging task
- Need – To automatically segment placenta in 3D (voxel-level classification) for qualitative and quantitative analysis
- Manual segmentation of the placenta is time-consuming and have high inter-observer and intra-observer variability
- Automatic 3D placenta segmentation could be used in clinical practice for monitoring conditions that result in pregnancy and birth complications such as PAS, fetal growth restriction, and suspicion of intrauterine fetal demise

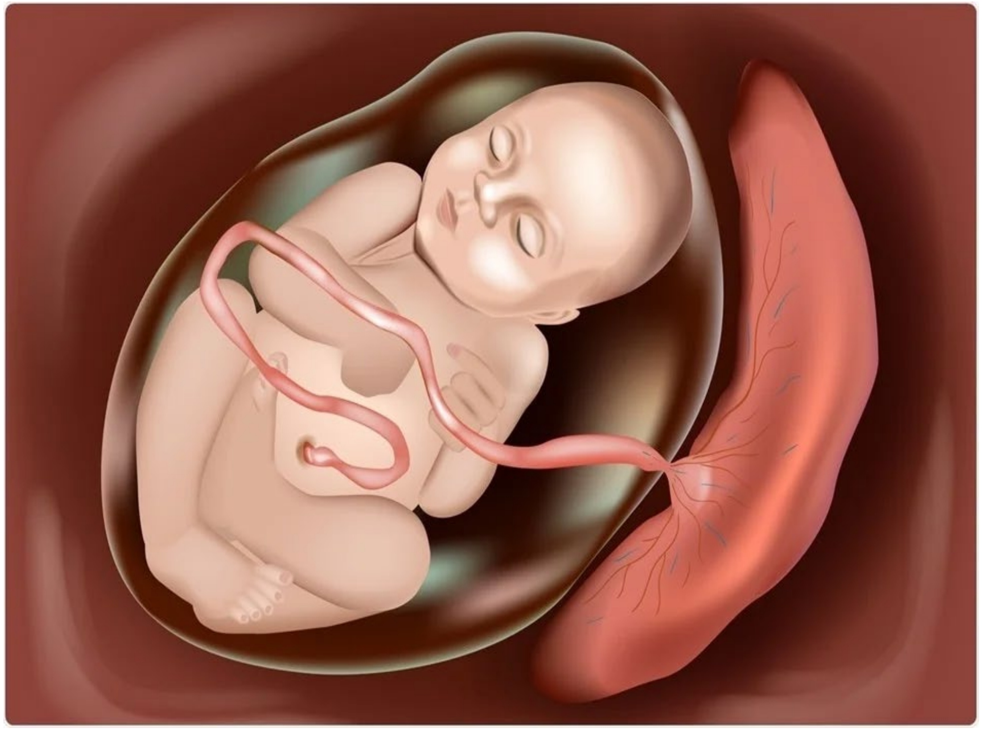

Image Source: Sakurra/Shutterstock.com
https://www.news-medical.net/news/20211116/SARS-CoV-2-replicates-in-human-placenta-with-release-of-infectious-viral-particles.aspx

Dataset

- Total 400 studies having Gray-scale (B-mode) and power doppler (PD) volumes are provided
- For ground-truth (GT) segmentation mask, manual annotation and the best 'threshold' images are computed using the following rules:
  - use same image in case there is only one annotated (segmented) image
  - compute intersection image (i.e., voxel-wise logical AND operation) in case there are two annotated (segmented) images
  - compute image based on majority voxel-wise voting in case there are three annotated (segmented) images

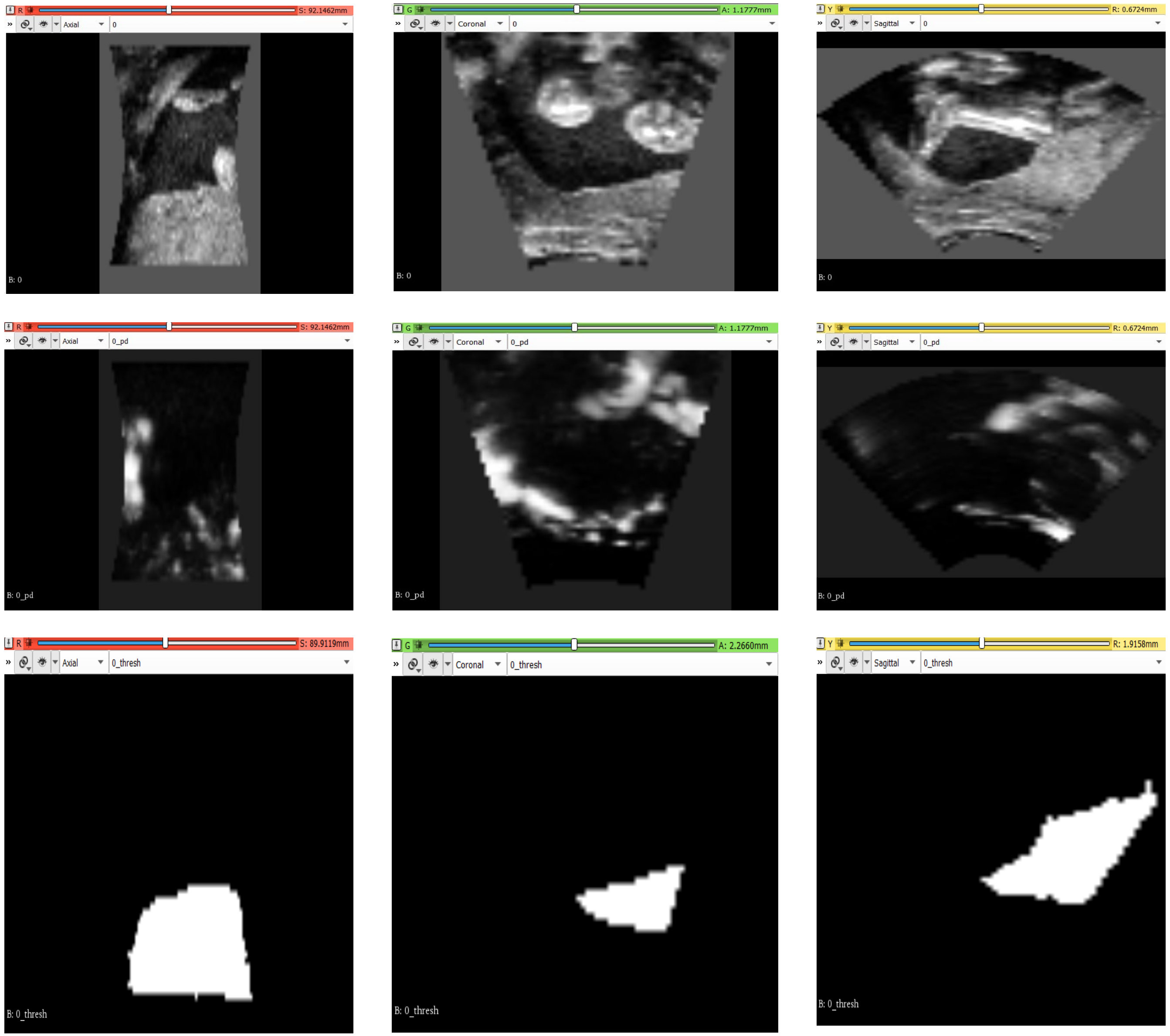

Dataset Pre-processing

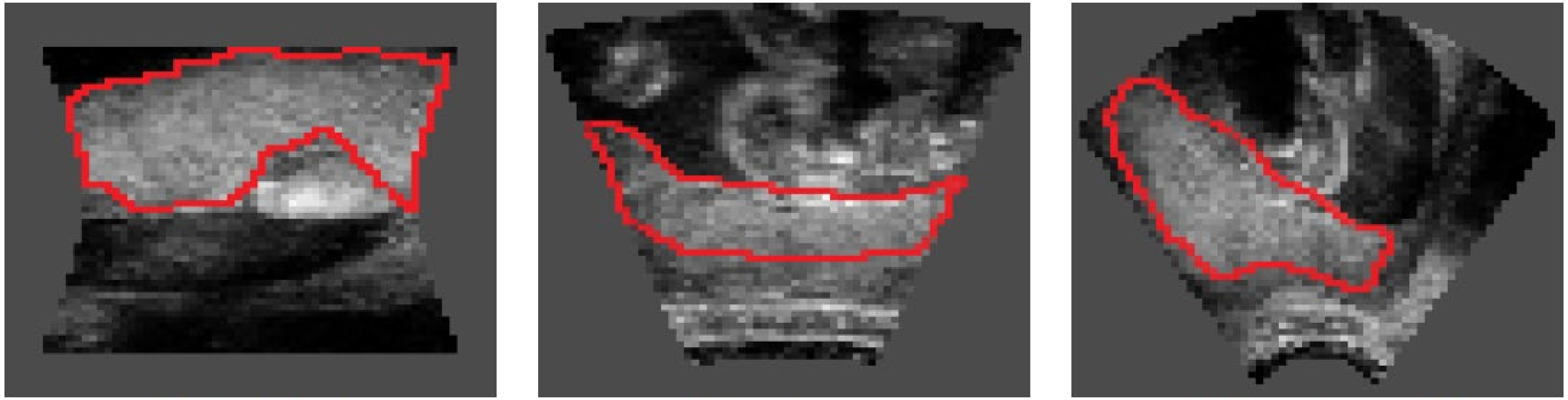

(a) B-mode Axial (b) B-mode Coronal (c) B-mode Sagittal

- Pre-processing needed to make data suitable for the framework.
- Pre-processing:
  - 3D volumes should be of same isotropic size (same size in x, y, z direction)
  - data to be provided in numbered format with each sample in folders from 0 to X, where X is the maximum number of studies
- All data (B-mode US, Power Doppler US, and annotated masks) were resized to 64 x 64 x 64
- B-mode and PD volumes are normalized by rescaling pixel values between range 0 to 255.

Singh *et al*., "Automatic 3D Multi-modal Ultrasound Segmentation of Human Placenta using Fusion strategies and Deep Learning", Ultrasound in Medicine and Biology, 2023 [Submitted]

Experimental setup

- Data split into training (60%), validation (20%), and testing (20%) without any data leakage (no patient overlap within sets)
- 400 studies divided as below:
  - training -> 240
  - validation -> 80
  - testing -> 80
- Data divided into 5 folds, keeping same ratio in each fold (240 training, 80 validation, and 80 testing)

Singh *et al*., "Automatic 3D Multi-modal Ultrasound Segmentation of Human Placenta using Fusion strategies and Deep Learning”, Ultrasound in Medicine and Biology, 2023 [Submitted]

Fusion strategies

- Early-fusion: concatenates original features at the input level
- Multi-stage or joint-fusion: concatenates extracted features
- Late-fusion: aggregates predictions at the decision level

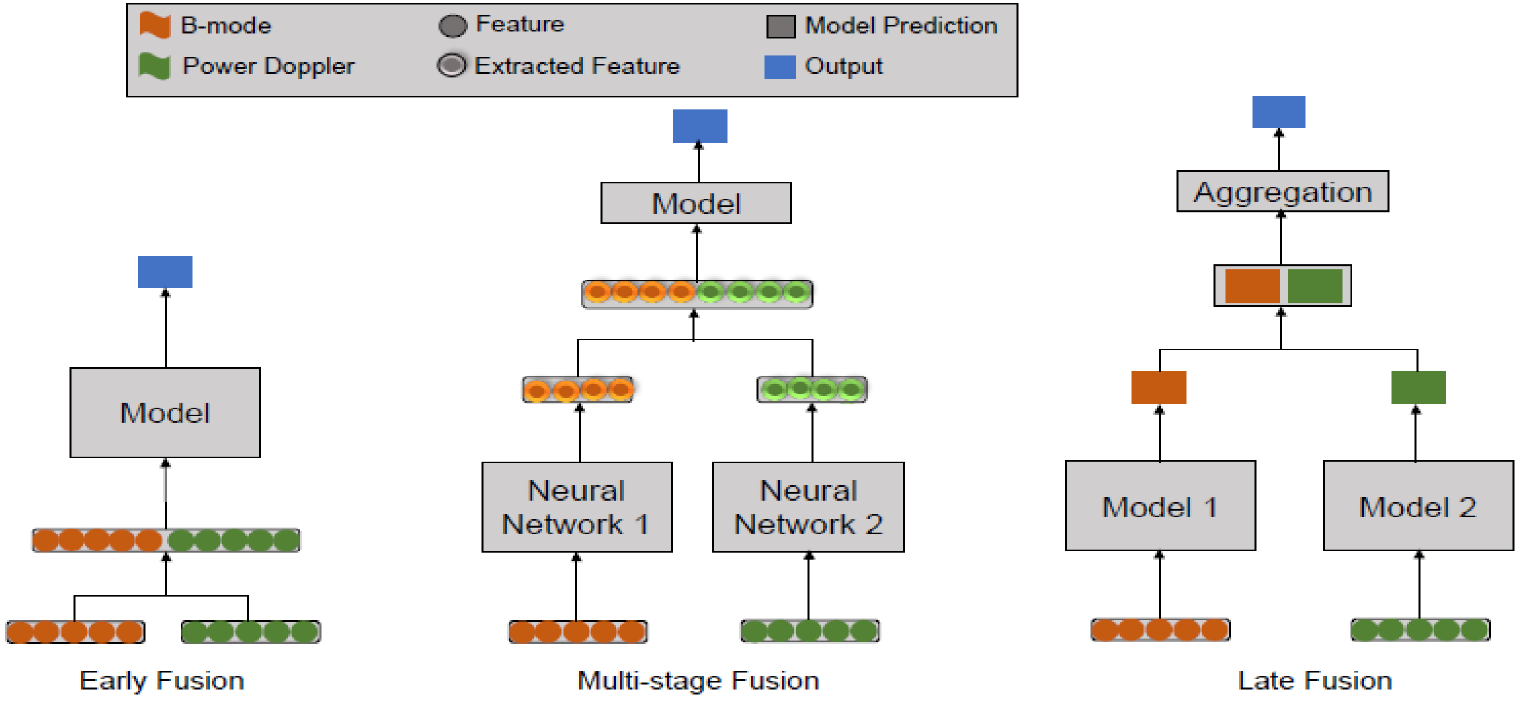

Singh *et al*., "Automatic 3D Multi-modal Ultrasound Segmentation of Human Placenta using Fusion strategies and Deep Learning", Ultrasound in Medicine and Biology, 2023 [Submitted]

Methodology

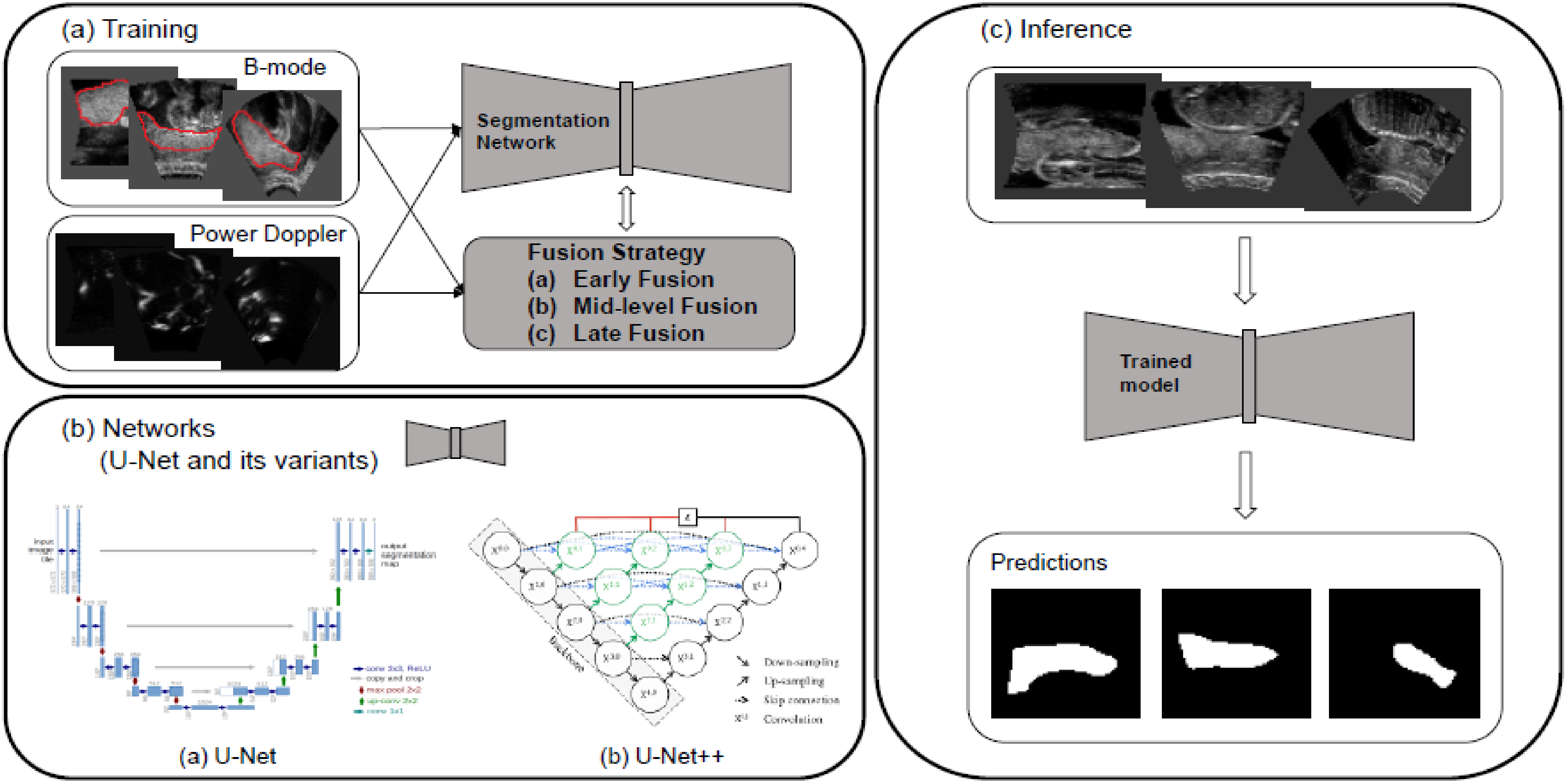

Results

Segmentation results comparing U-Net model performance for five folds of the final dataset with each fold having #train=240, #validation=80, and #test=80 3D ultrasound volumes. Results are averaged values over all studies in the test set with ± standard deviation of metric for that test set.

Fold# (Dataset)	DSC	Jaccard Index	HD (mm)	MSD (mm)
Fold 1	0.823 ± 0.101	0.708 ± 0.102	8.645 ± 6.322	1.501 ± 0.454
Fold 2	0.825 ± 0.058	0.706 ± 0.076	7.920 ± 4.665	1.595 ± 0.631
Fold 3	0.823 ± 0.064	0.704 ± 0.082	10.500 ± 6.111	1.664 ± 0.887
Fold 4	0.814 ± 0.075	0.692 ± 0.093	7.978 ± 4.839	1.722 ± 0.912
Fold 5	0.821 ± 0.045	0.698 ± 0.062	8.262 ± 4.420	1.572 ± 0.408

Segmentation results comparing U-Net++ model performance for five folds of the final dataset with each fold having #train=240, #validation=80, and #test=80 3D ultrasound volumes. Results are averaged values over all studies in the test set with ± standard deviation of metric for that test set.

Fold# (Dataset)	DSC	Jaccard Index	HD (mm)	MSD (mm)
Fold 1	0.828 ± 0.076	0.706 ± 0.067	4.898 ± 3.156	1.196 ± 0.752
Fold 2	0.819 ± 0.042	0.694 ± 0.113	7.348 ± 5.245	2.039 ± 0.574
Fold 3	0.824 ± 0.056	0.700 ± 0.018	7.615 ± 4.758	1.502 ± 0.626
Fold 4	0.833 ± 0.107	0.715 ± 0.045	4.690 ± 3.167	1.340 ± 0.285
Fold 5	0.840 ± 0.072	0.725 ± 0.057	4.123 ± 3.032	1.177 ± 0.377

Singh *et al*., "Automatic 3D Multi-modal Ultrasound Segmentation of Human Placenta using Fusion strategies and Deep Learning", Ultrasound in Medicine and Biology, 2023 [Submitted]

Results

Segmentation results with and without data augmentation. Results are averaged values over all studies in the test set with ± standard deviation of metric for that test set.

Method	DSC	Jaccard Index	HD (mm)	MSD (mm)
U-Net, without data augmentation	0.824	0.700	7.615	1.502
U-Net, with data augmentation	0.833	0.714	4.690	1.340
U-Net++, without data augmentation	0.839	0.722	7.141	1.279
U-Net++, with data augmentation	0.847	0.725	4.123	1.177

Segmentation results applying applying early fusion, intermediate fusion, and late fusion for the two modalities, namely, B-mode and Power Doppler 3D ultrasound volumes. Results are averaged values over all studies in the test set with ± standard deviation of metric for that test set.

Method	DSC	Jaccard Index	HD (mm)	MSD (mm)
Early fusion (U-Net, without data augmentation)	0.831	0.711	8.944	1.078
Intermediate fusion (U-Net, without data augmentation)	0.825	0.702	5.196	1.484
Late fusion (U-Net, without data augmentation)	0.818	0.693	9.110	1.582
Early fusion (U-Net++, without data augmentation)	0.847	0.725	4.472	1.137
Intermediate fusion (U-Net++, without data augmentation)	0.831	0.710	5.830	1.442
Late fusion (U-Net++, without data augmentation)	0.826	0.704	16.643	1.229
Early fusion (U-Net, with data augmentation)	0.838	0.722	4.898	1.144
Intermediate fusion (U-Net, with data augmentation)	0.829	0.708	7.071	1.818
Late fusion (U-Net, with data augmentation)	0.822	0.698	7.549	2.229
Early fusion (U-Net++, with data augmentation)	0.849	0.738	4.051	1.007
Intermediate fusion (U-Net++, with data augmentation)	0.839	0.722	7.141	1.279
Late fusion (U-Net++, with data augmentation)	0.835	0.717	10.295	1.025

Qualitative Results

- DSC: 0.7135
  Jaccard Index: 0.5546
  Hausdorff Distance (HD95): 9.4339
  MSD: 304.4385

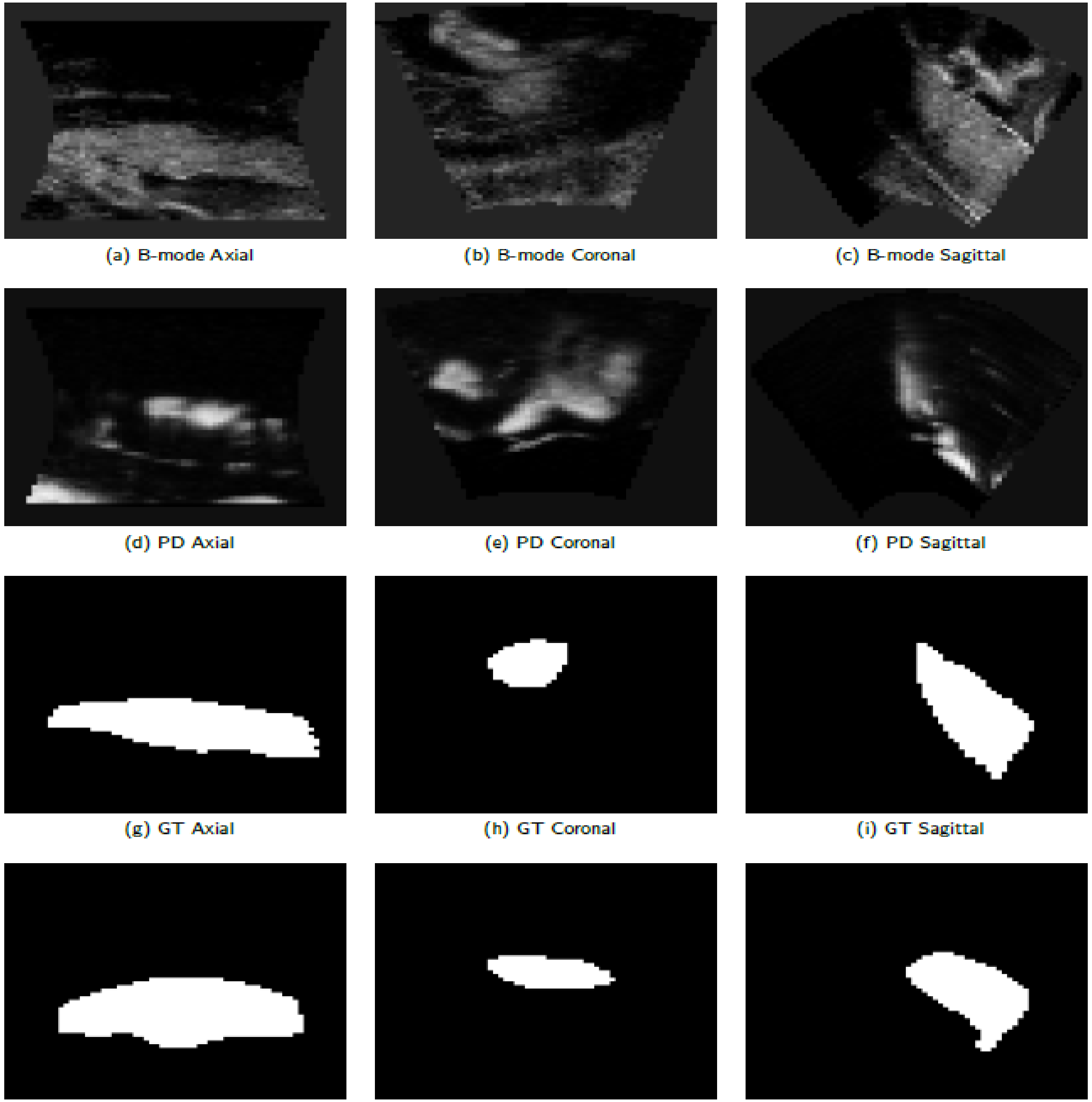

(a) B-mode Axial (b) B-mode Coronal (c) B-mode Sagittal
(d) PD Axial (e) PD Coronal (f) PD Sagittal
(g) GT Axial (h) GT Coronal (i) GT Sagittal
(j) Predicted Axial (k) Predicted Coronal (l) Predicted Sagittal

Singh *et al*., "Automatic 3D Multi-modal Ultrasound Segmentation of Human Placenta using Fusion strategies and Deep Learning", Ultrasound in Medicine and Biology, 2023 [Submitted]

Qualitative Results

- DSC: 0.9039

  Jaccard Index: 0.8247

  Hausdorff Distance (HD95): 3.0000

  MSD: 0.7189

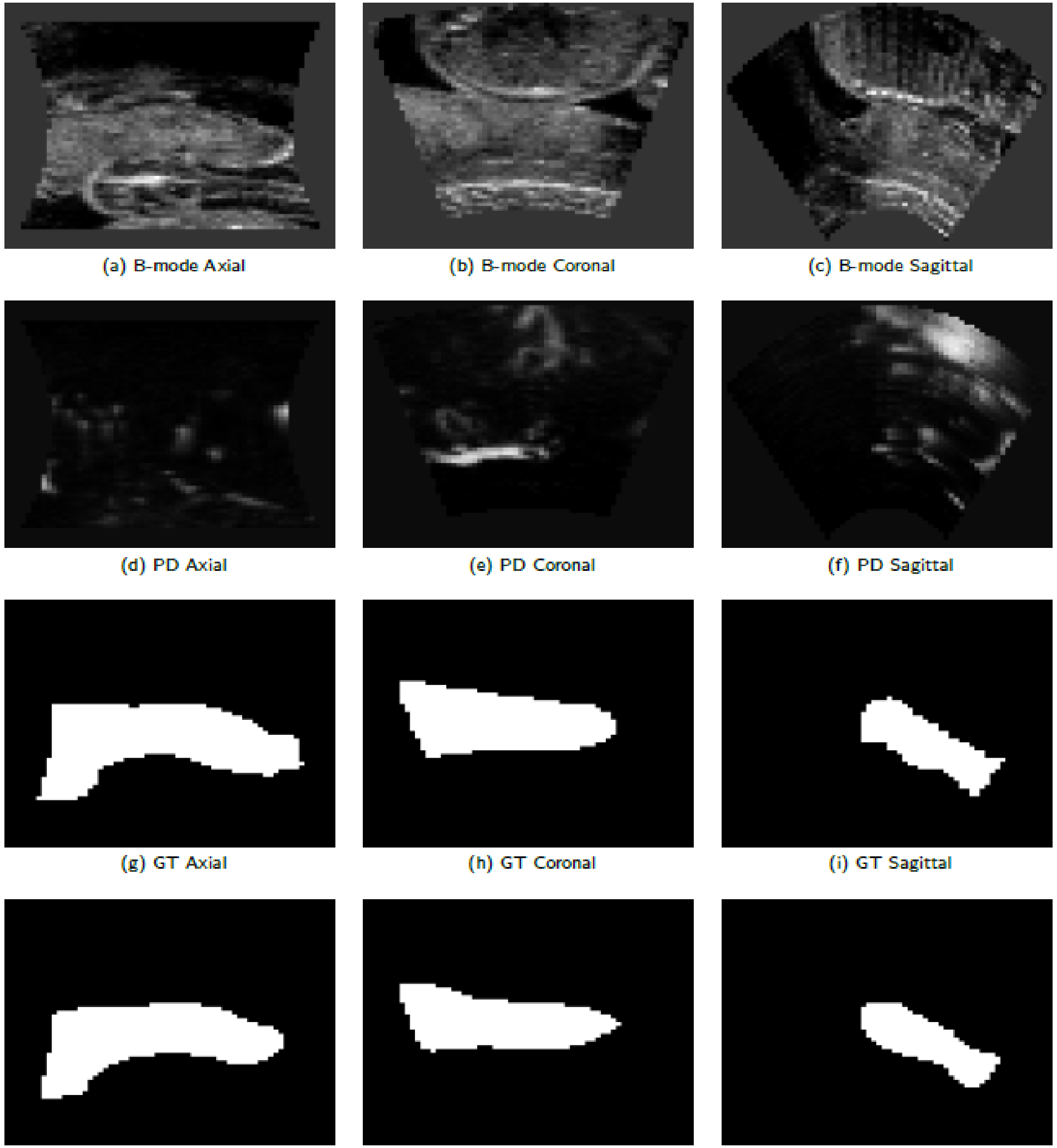

(a) B-mode Axial (b) B-mode Coronal (c) B-mode Sagittal (d) PD Axial (e) PD Coronal (f) PD Sagittal (g) GT Axial (h) GT Coronal (i) GT Sagittal (j) Predicted Axial (k) Predicted Coronal (l) Predicted Sagittal

Next steps – Whole placenta segmentation

- Placenta size grows with the gestation age
- It is hard to capture entire placenta at late gestation
  - Limited field-of-view (FOV)
  - A single US probe have too small FOV to capture the whole placenta
- The Need – Stitching
  - The entire placenta can be captured by acquiring, aligning, and stitching multiple 3D US images to get large FOV

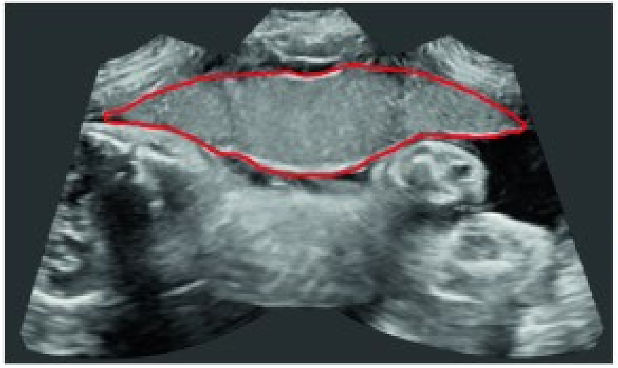

Estimated gestational age (weeks)	Mean±SD	
	Placenta thickness (mm)	Estimated fetal weight (g)
15	22.6±2.5	147.0±16.5
16	22.5±1.9	181.5±17.4
17	26.0±0.0	212.5±0.0
18	24.0±0.2	233.3±40.0
19	27.6±2.8	330.5±21.7
20	29.1±5.6	357.8±31.2
21	27.8±4.9	421.7±36.5
22	31.5±5.2	542.5±63.9
23	31.2±3.4	599.8±65.2
24	31.9±3.9	691.5±64.6
25	30.7±2.7	805.3±46.0
26	33.2±3.4	963.5±68.9
27	34.0±3.2	1063.7±66.8
28	34.0±2.2	1235.2±69.2
29	35.5±4.9	1375.9±79.3
30	38.9±5.9	1539.3±211.9
31	36.0±5.3	1617.0±137.0
32	33.5±3.5	1766.6±206.7
33	38.8±6.4	2148.1±202.7
34	39.0±5.3	2348.1±106.1
35	41.4±11.6	2292.4±764.9
36	40.9±7.2	2710.0±275.2
37	40.1±4.8	2884.8±251.6
38	38.5±2.5	3148.4±505.4
39	39.3±4.4	3187.4±305.4
40	39.3±5.7	3304.8±284.6

SD: Standard deviation

Source: Adeyekun et al. (2015). Relationship between 2-D ultrasound measurement of placental thickness and estimated fetal weight.
Image source: Zimmer et al. (2019). Towards Whole Placenta Segmentation at Late Gestation using multi-view US images. MICCAI.

Whole placenta segmentation

- ➢ Placenta size grows with the gestation age

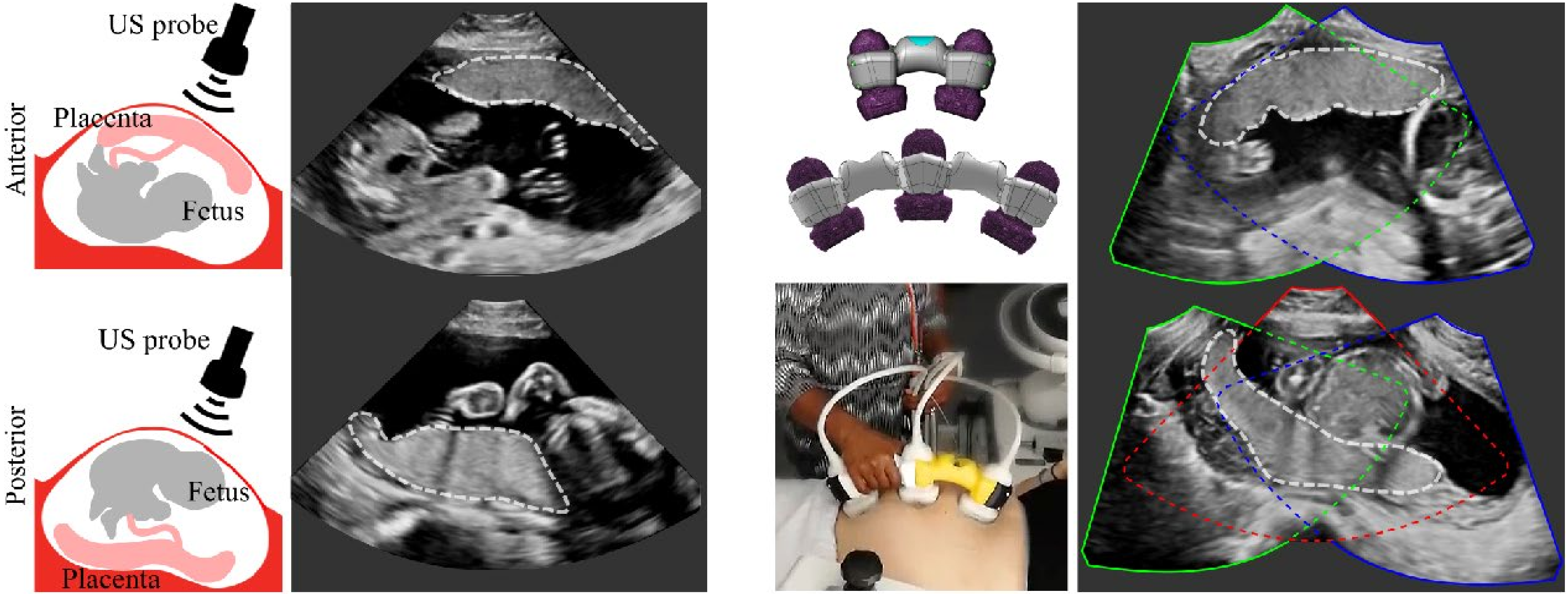

(a) Single US images

(b) Multi-view US images

Other Medical Imaging and Informatics projects

Automated Extraction of ARPD from lung MDCT Images

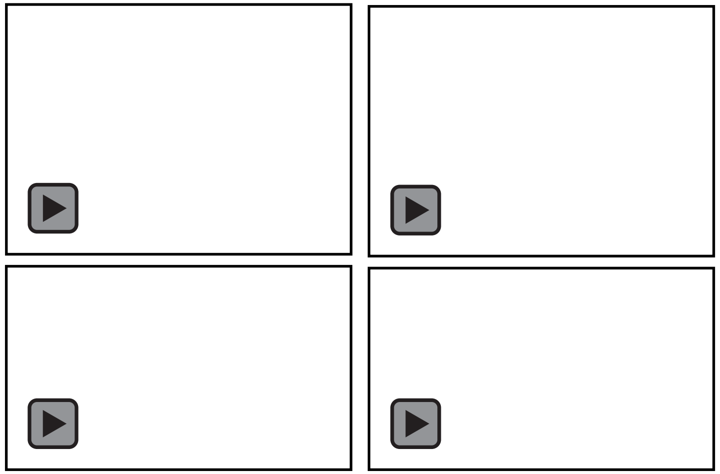

Analysis and Enhancement of MR Neuroimages

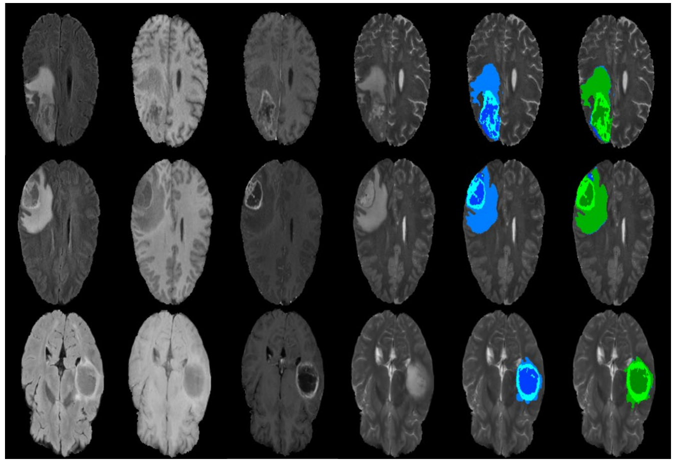

Diagnosis of Neurodegenerative disease using Deep Multimodal Analysis

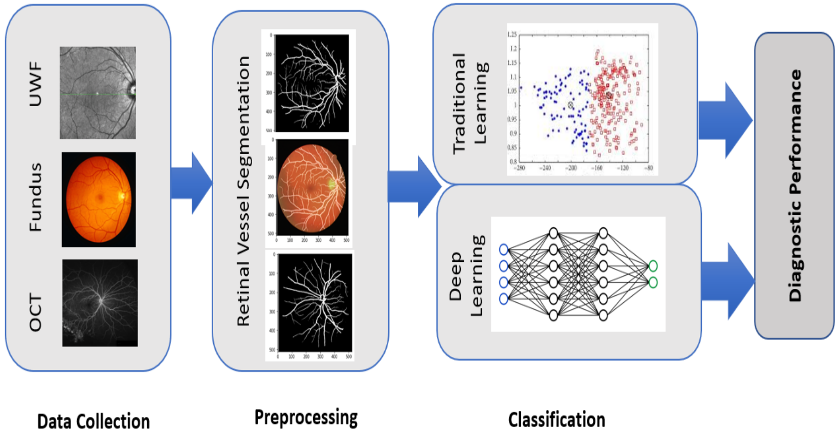

Training Radiomics-based CNNs for Clinical Outcome Prediction

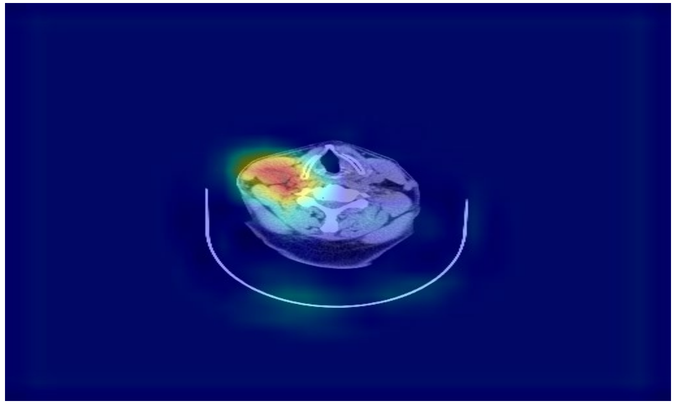

Medical Visual Question Answering (Med-VQA)

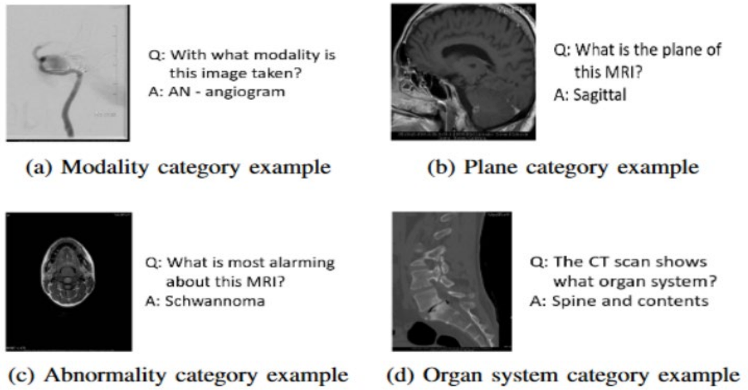

Early Detection of Alzheimer's Disease using ML

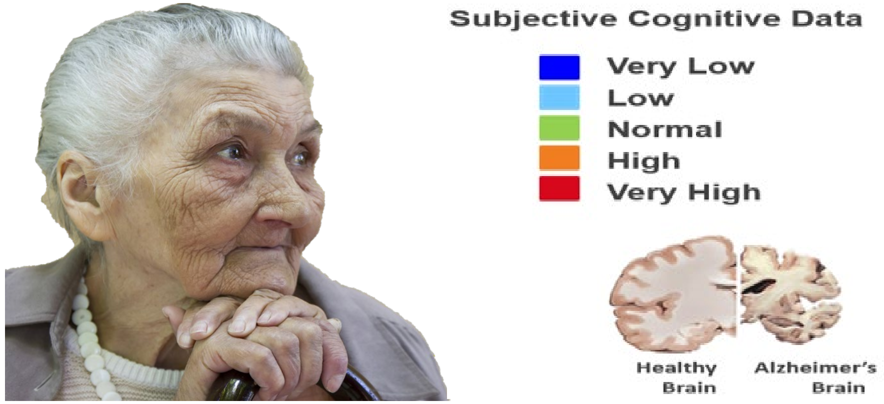

*Projects shown are undertaken by PhD, MPhil and Hons Thesis candidates and are supervised by academics in Computer Vision group at UNSW CSE in collaboration with clinical collaborators.

Other Medical Imaging and Informatics projects

Vertebral Compression Fracture (VCF) Detection in CT images

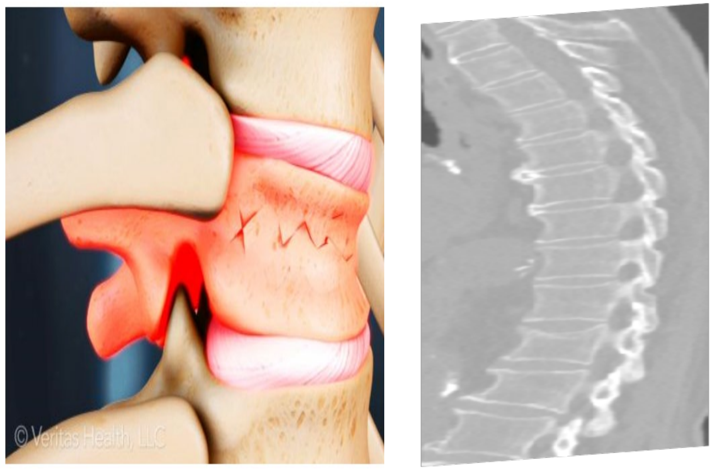

Prostate Segmentation from MR Images

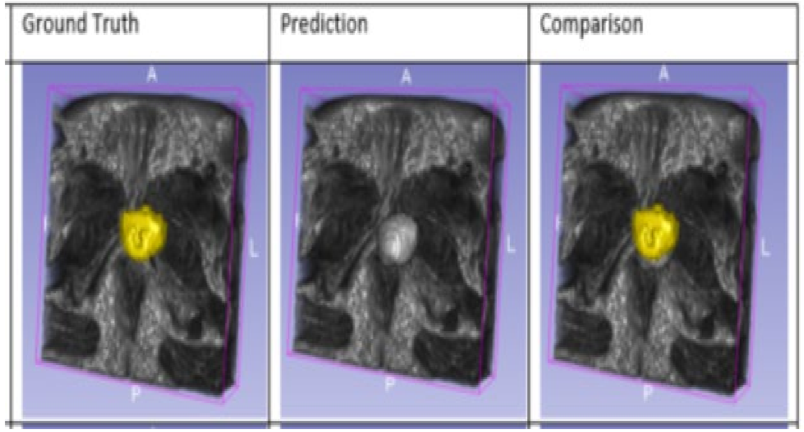

Multimodal Severity Detection for Black Lung Disease

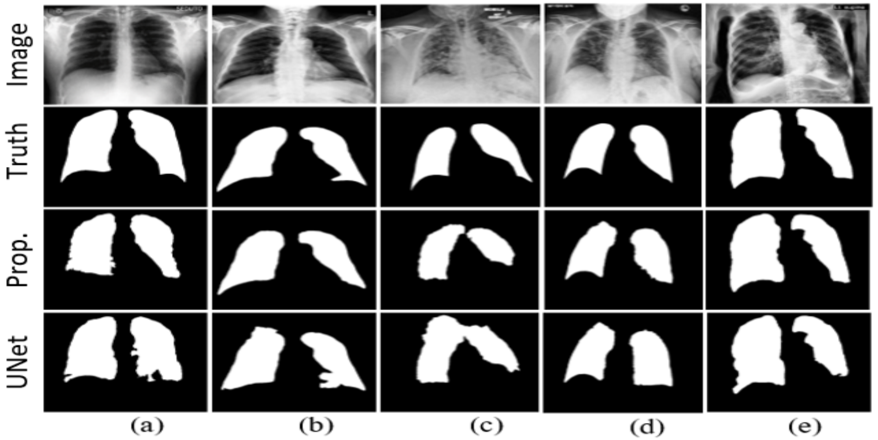

Quantification and Severity Estimation of Acute Diverticulitis

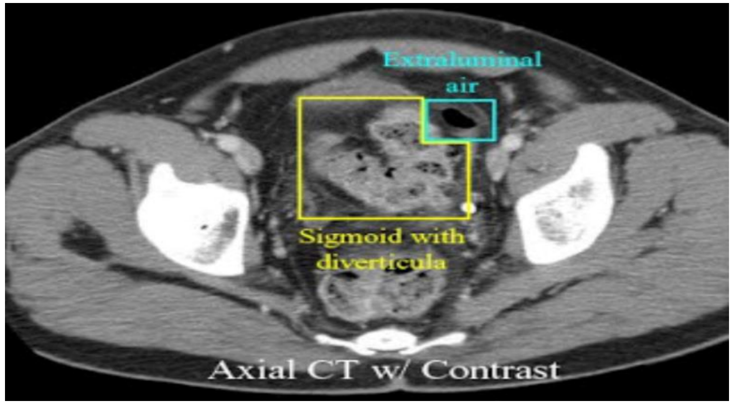

Automated Segmentation of Coronary Arteries

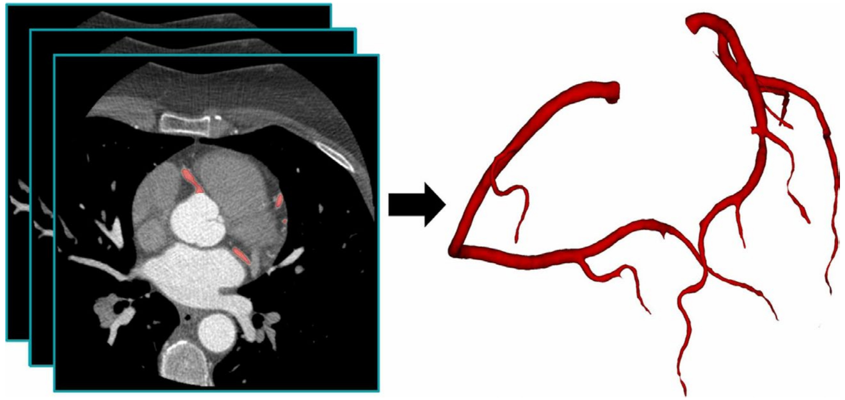

Multi-organ and Tumor Segmentation from Abdominal CT images

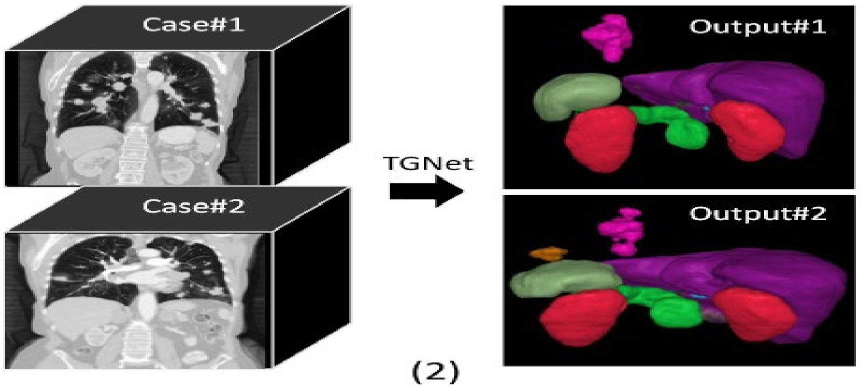

*Projects shown are undertaken by PhD, MPhil and Hons Thesis candidates and are supervised by academics in Computer Vision group at UNSW CSE in collaboration with clinical collaborators.

Concluding Remarks

- Computational methods have an increasing role in medical imaging
- **Challenges**
  - big raw data but limited curated data
  - combining imaging and non-imaging data
  - data visualisation
  - moving from 2D to 3D
  - explainable and interpretable models
  - ethical and legal dilemmas

Collaborators

Arcot Sowmya
Professor and Head, School of Computer Science and Engineering
UNSW

Erik Meijering
Professor, Biomedical Image Computing
UNSW

Dr Gihan Samarasinghe
Postdoctoral Researcher

Manna Elizabeth Philip
PhD Student

Dr Banafsheh Pazokifard
Alumnus MIA group

Upul Senanayake
PhD Student

Sankaran Iyer
PhD Student

Dr Daniel Moses
Director, Medical Imaging, PoWH

Annette Spooner
PhD Student

Jian Kang
PhD Student

Dr Laughlin Dawes
Consultant Radiologist, PoWH

Collaborators

Prof Alec Welsh
Royal Hospital for Women/School of Women's and Children's Health, UNSW

Dr Gordon Stevenson
School of Women's and Children's Health UNSW

Scientia Prof Perminder Sachdev
Co-director, Centre for Healthy Brain Ageing, School of Psychiatry, UNSW and Clinical Director, Neuropsychiatric Institute, PoWH

A/Prof Wei Wen
Centre for Healthy Brain Ageing, School o Psychiatry, UNSW/Neuropsychiatric Institu PoWH

Dr Nicole Kochan
Centre for Healthy Brain Ageing, School of Psychiatry, UNSW

Dr Christopher White
Director Research, SESLHD/Dept of Clinica Chemistry and Endocrinology, PoWH

Collaborators

Kuruparan shanmugalingam
PhD Student

Louisa Canepa
Honors Thesis Student

Mina Ghaffari
PhD Student

Dr. Praveen Ravindran
Colorectal & Robotic Surgeon
Australian Robotic Colorectal Surgery
AMO Sydney Adventist Hospital

Collaborators

Mahmudul Hasan
PhD Student

Akizur Rahman
PhD Student

Sonit Singh
Postdoctoral Fellow

Shariful Alam
PhD Student

References

[1] Aleksander Sizarov and Younes Boudjemline, “Valve interventions in utero: Understanding the timing, indications, and approaches,” Canadian Journal of Cardiology, vol. 33, no. 9, pp. 1150–1158, 2017.

[2] M. E. Philip, A. Sowmya, H. Avnet, A. Ferreira, G. Stevenson and A. Welsh, "Convolutional Neural Networks for Automated Fetal Cardiac Assessment using 4D B-Mode Ultrasound," 2019 IEEE 16th International Symposium on Biomedical Imaging (ISBI 2019), Venice, Italy, 2019, pp. 824-828.

[3] B. Messing, Y. Gilboa, M. Lipschuetz, D. V. Valsky, S. M. Cohen And S. Yagel, “Fetal tricuspid annular plane systolic excursion (f-TAPSE): evaluation of fetal right heart systolic function with conventional M-mode ultrasound and spatiotemporal image correlation (STIC) M-mode”, Ultrasound Obstetrics & Gynecology; vol: 42: 182–188, 2013.

[4] R. J. Schneider, D. P. Perrin, N. V. Vasilyev, G. R. Marx, P. J. Del Nido, and R. D. Howe, “Mitral annulus segmentation from four-dimensional ultrasound using a valve state predictor and constrained optical flow,” Med. Image Anal., vol. 16, no. 2, pp. 497–504, 2012.

[5] C. Sardsud, S. Auephanwiriyakul, N. Theera-Umpon, and T. Tongsong, “Patch-Based Fetal Heart Chamber Segmentation in Ultrasound Sequences Using Possibilistic Clustering,” Proc. Int. Conf. Comput. Intell. Model. Simul., vol. 2016–Septe, pp. 43–48, 2016.

[6] L. Yu, Y. Guo, Y. Wang, S. Member, J. Yu, and P. Chen, “Segmentation of Fetal Left Ventricle in Echocardiographic Sequences Based on Dynamic Convolutional Neural Networks,” vol. 9294, no. c, 2016.

[7]. Grishick et al. (2014). Rich Feature Hierarchies for Accurate Object Detection and Semantic Segmentation. CVPR 2014

[8]. Grishick, Ross. (2015). Fast R-CNN. ICCV 2015.

[9]. Sen et al. (2015). Faster R-CNN: Towards Real-Time Object Detection with Region Proposal Networks. NeurIPS 2015.

[10] Olaf Ronneberger, Philipp Fischer, and Thomas Brox,“U-Net: Convolutional Networks for Biomedical Image Segmentation,” International Conference on Medical Image Computing and Computer-Assisted Intervention. (MICCAI), pp. 234–241, 2015.

[11] M. E. Philip *et al.*, "A Machine Learning Framework for Fully Automatic 3D Fetal Cardiac Ultrasound Evaluation," *2022 IEEE 19th International Symposium on Biomedical Imaging (ISBI)*, 2022, pp. 1-5, doi: 10.1109/ISBI52829.2022.9761613.

[12]. Singh et al., “Automatic 3D Multi-modal Ultrasound Segmentation of Human Placenta using Fusion strategies and Deep Learning”, Ultrasound in Medicine and Biology, 2023 [Under Review].

[13]. Zimmer et al. (2023). Placenta Segmentation in Ultrasound Imaging: Addressing Sources of Uncertainty and Limited Field-of-View. Medical Image Analysis. 2023.

Questions?